University of Durham

Department of Mathematical Sciences

Modelling the Indian Drum

Author:
James Hagues

Supervisor:
Dr. Bernard Piette

April 30, 2010

Abstract

This project studies a number of different drum models and finds the frequencies of their vibrational modes. The standard drum is investigated, along with the Indian drum called the tabla. A tabla consists of the right-handed, concentrically loaded drum and the left-handed, eccentrically loaded drum. Two and three-density models are used to approximate the right-handed tabla and the three-density model is found to produce eigenfrequencies that have very good agreement with experimental values. The effect of damping on the drum is also calculated and a different method for solving the two-density model is investigated, which can also be used to solve the left-handed drum.

Acknowledgements

I would like to thank Dr. Bernard Piette for his help and direction during the writing of this project.
Additionally, I would like to thank Johnny for computer-sitting lengthy Maple runs and Marty and Hannah for proof-reading the project.

Contents

Chapter 1

Introduction

The Tabla is a precussion instrument that originates from northern India and consists of two drums. The instrument has widespread use within both classical and popular music and is comprised of a pair of small drums that are played by striking the membrane with the hand. The tabla is shown in Figure 1.1 .

Figure 1.1: The tabla[1]. The right-handed drum is on the left and the left-handed drum is on the right.

1.1 The Tabla

The precise origins of the tabla are unclear but it is thought to have evolved in the 18^{th} century. The older instruments of the pakhawaj and mridangam are believed to have influenced its development. These drums have a membrane with properties that are similar to the tabla.

The two drums that make up the tabla have many common characteristics, but also distinct differences. The right-handed drum is called the tabla and the left-handed drum is called the dāyāñ. Both drums have a membrane that is made from goatskin. Upon the edge of this membrane an outer halo of skin is placed. This is made from a different skin, commonly

[1]Image from http://artdrum.com/

a cow's or a buffalo's, and is known as the 'Chati'. In addition to this, a loaded region known as the 'Syahi', is added to the middle of the membrane [CT]. The special properties of the tabla result mainly from the contribution of the syahi. It gives the central area of the membrane a significantly greater radial density than the surrounding membrane. The syahi consists of a combination of flour, water, and a mixture made from iron and other substances. It is constructed by adding thin layers of this mixture to the drum membrane and is crucial for creating the tone quality of the instrument. The successive layers are initially applied with a constant radius, then the radius of application is gradually reduced to the smallest radius of application of about a centimeter. This process is repeated a few times creating a thickness gradient within the syahi [CK]. This can clearly be seen in Figure 1.2 . The construction process means the difference in thickness between the six or seven layers within the syahi are much smaller than the difference in thickness between the edge of the syahi and the membrane. Ramakrishna and Sondhi [RS] give experimental values (stated later in Section 3.2.1) for the density ratio and the radius ratio between the two regions of the tabla in normal use.

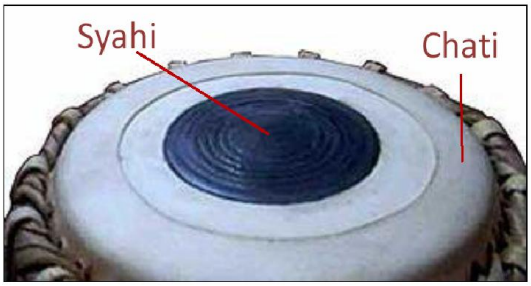

Figure 1.2: The membrane of the tabla with the syahi and chati labelled[2]. The picture shows that the thickness of the syahi is not constant.

Despite these similarities, the two drums differ in construction. The circular loaded region of the right-handed drum is concentrically placed, whereas the loaded portion of the left-handed drum has an off-centre position (as seen in Figure 1.1). The shell of the right-handed drum is constructed from wood, normally rosewood, and is hollow for approximately half its depth. In contrast, the shell of the left-handed drum is commonly made from a metal, preferably brass or copper, although it is sometimes shaped from wood or clay. The left-handed drum is also significantly larger than the right-handed drum.

Ramakrishna and Sondhi [RS] list the fundamental frequency of the right-handed tabla as between 110Hz and 200Hz. Experiments carried out by Kapur [K] find the fundamental frequency of the tabla used in his experiment to be 172Hz, which corresponds to the F below middle C. In this work the exact frequency of F_3 to 4 significant figures, 174.6 Hz, will be used. The left-handed tabla is normally tuned to the fourth or fifth below the right-handed (frequencies 116.5 Hz and 130.8 Hz) [TT]. Tuning of the tabla is achieved by altering the tension of the membrane. A wooden peg, located between the straps that hold the membrane and the shell together, can be moved up and down to tighten or slacken the membrane. Fine tuning is attained by striking the braided ring around the membrane with a hammer.

[2]Image from Wikimedia Commons and edited using Microsoft Powerpoint

The technique used in playing the tabla can greatly affect the sound that is produced. There are twelve basic tabla strokes involving different methods for striking the membrane and all have distinct sounds and tone qualities [CKT].

Much of the early scientific work on the Tabla was undertaken by the nobel laureate Sir Chandrasekhara Venkata Raman. His investigations showed that the overtones of the tabla were harmonic and degenerate.

1.2 The Harmonicity of the Tabla

If a note is played on an instrument then additional vibrations at higher frequencies are produced alongside the fundamental frequency (the pitch of the note). The human ear perceives these as one note instead of hearing the harmonics separately. This constructs the tone quality of the instrument. If an instrument is perfectly harmonic, the harmonics are in integer multiples of the fundamental frequency. This can be described in the following equation where f_h is the harmonic frequency and f_0 is the fundamental frequency:

$$f_h = nf_0 \qquad \text{with} \qquad n = \{1, 2, ...\} \ . \tag{1.1}$$

A perfectly harmonic instrument sounds pleasing to the human ear because it replicates the harmonics that are naturally produced by the human voice. An example of a harmonic instrument is a violin or a flute. If an instrument is inharmonic, like an ordinary drum, then the harmonics bear no relation to the integer ratio.

Raman's experiments revealed the harmonic properties of the tabla. He found that a number of the vibrational modes of the tabla share the same frequency, all of which are close to perfectly harmonic frequencies. These degenerate modes do not appear in the ordinary drum. Raman also found that the 6^{th} harmonic and any higher harmonics are sufficiently damped so that their contribution to the tone of the instrument is insignificant [IMD]. If these higher harmonics did contribute to the tabla's tone then their effect could only be detrimental to the tuning of the tabla's harmonics as this would mean that a greater number would require tuning.

The damping of the higher harmonics is achieved by the outer halo of skin (Chati). The ampliltudes of vibration of the higher frequency harmonics are greater towards the edge of the drum than those of the lower harmonics, relative to the amplitudes of the respective vibrations near the centre (see Section 4.1). The damping effect of the Chati is therefore much greater at higher frequencies while lower frequencies are comparatively uninfluenced.

Experiments carried out by Ramakrishna and Sondhi give values to the relative frequencies of the harmonics for the right-handed tabla (Table 1.1). They state that the drummer tunes to the second harmonic so this is the frequency that is used to calculate the relative frequencies. The different modes of vibration are explained in more detail later on (Section 2.2) but are denoted ψ_{nj} , where n is the order and j is the root. As n and j increase, the frequency of the mode increases. The different modes are excited with varying amplitudes of vibration depending on where the membrane is struck. A strike near the edge of the drum will excite the higher modes of vibration more than a strike at the centre.

The different strikes that are used by tabla players are called 'notes'. Different notes are produced by strikes in different locations. Also, a number of strikes involve lightly touching the membrane with a finger other than the striking finger to prevent some vibrational modes.

	Frequency ratio	
Mode	Tabla in normal use	Same Tabla with opened shell
ψ_{01}	1.10	1.03
ψ_{11}	2.00	2.00
ψ_{02}	3.00	3.00
ψ_{21}	3.00	3.00
ψ_{12}	4.01	4.00
ψ_{31}	4.03	4.00
ψ_{41}	5.07	5.03
ψ_{22}	5.07	5.08
ψ_{03}	5.11	5.04

Table 1.1: Table showing the relative frequency of the modes of vibration of the right-handed tabla, taken from Rama. and Sondhi [RS]. The 2^{nd} harmonic is defined as 2.00.

The models that will be produced in this work will not take into account the effect of the air pressure within the shell, so the frequency values from the open shell are more relevant to the subsequent models. These are also notably closer to the integer ratios.

Chapter 2

The Model of an Ordinary Drum

To mathematically find the allowed frequencies of vibration for a drum, the wave equation must be solved. The wave equation describes the propagation of a wave over time and takes the form of a second order partial differential equation.

Initially the wave equation will be solved for an ordinary drum, modelled as a one-density membrane. The method is described in 'Music: A Mathematical Offering', written by D. Benson [B].

2.1 Solving the wave equation

The wave equation is given by

$$\frac{\partial^2 z}{\partial t^2} = c^2 \nabla^2 z \,, \qquad \text{with} \qquad c = \sqrt{\frac{T}{\rho}} \,. \tag{2.1}$$

z is the displacement of the medium from its equilibrium position, c is the propagation speed of the wave and T and ρ are the tension and density of the medium. The membrane of the drum is taken to be within the region of radius $0 \leq r \leq a$ and a number of boundary conditions for the drum are imposed on the equation. The displacement must be finite within the drum membrane and at the edge of the drum there is no displacement. Additionally, the displacement is 2π periodic with respect to θ. These boundary conditions are stated mathematically as

$$z(r) \in \mathbb{R} \qquad \text{when} \qquad 0 \leq r \leq a \,, \tag{2.2}$$

$$z(r) = 0 \qquad \text{when} \qquad r = a \,, \tag{2.3}$$

$$z(\theta) = z(\theta + 2\pi n) \,. \tag{2.4}$$

As the boundary conditions in the case of the drum depend upon the radius of the drum and the angular coordinate θ polar coordinates are used as the coordinate system (shown

in Figure 2.1). The Laplacian must therefore be of polar coordinate form, resulting in the wave equation being expressed as

$$\frac{\partial^2 z}{\partial t^2} = c^2 \left(\frac{\partial^2 z}{\partial r^2} + \frac{1}{r}\frac{\partial z}{\partial r} + \frac{1}{r^2}\frac{\partial^2 z}{\partial \theta^2} \right) . \tag{2.5}$$

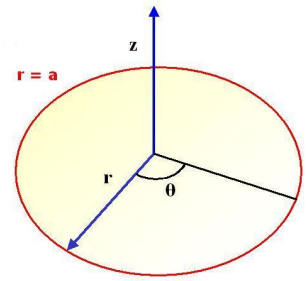

Figure 2.1: The axes of the coordinate system of the drum with radius a [3]

The solution to the wave equation will be in the form of a separable solution $z(r, \theta, t) = f(r)\, g(\theta)\, h(t)$. If this is substituted into equation (2.5) then it becomes

$$f(r)\, g(\theta)\, h_{tt}(t) = c^2 \left(f_{rr}(r)\, g(\theta)\, h(t) + \frac{1}{r} f_r(r)\, g(\theta)\, h(t) + \frac{1}{r^2} f(r)\, g_{\theta\theta}(\theta)\, h(t) \right) . \tag{2.6}$$

To separate the variables both sides are now divided by $f(r)\, g(\theta)\, h(t)$:

$$\frac{h_{tt}(t)}{h(t)} = c^2 \left(\frac{f_{rr}(r)}{f(r)} + \frac{1}{r}\frac{f_r(r)}{f(r)} + \frac{1}{r^2}\frac{g_{\theta\theta}(\theta)}{g(\theta)} \right) . \tag{2.7}$$

The left-hand side of this equation depends only on the variable t and the right-hand side depends only on the variables r and θ. As each side of the equation depends on different independent variables, the value of each side must be independent of all the variables, and therefore a constant. The choice shall be made to call this constant k_1 , giving

$$\boxed{\frac{h_{tt}(t)}{h(t)} = c^2 \left(\frac{f_{rr}(r)}{f(r)} + \frac{1}{r}\frac{f_r(r)}{f(r)} + \frac{1}{r^2}\frac{g_{\theta\theta}(\theta)}{g(\theta)} \right) = k_1 .} \tag{2.8}$$

The equation that must be solved to find $h(t)$ is therefore

$$h_{tt}(t) = k_1 h(t) . \tag{2.9}$$

The general solution to this is

$$h(t) = B_1 e^{\sqrt{k_1} t + \kappa_1} + B_2 e^{-\sqrt{k_1} t + \kappa_2} . \tag{2.10}$$

[3] Image created using Microsoft Powerpoint

A drum produces a note and therefore oscillates. To create oscillations the system needs to be underdamped, requiring the condition $k_1 < 0$ to hold, giving $k_1 = -\omega^2$ and

$$h(t) = B_1 e^{i(\omega t+\varphi_1)} + B_2 e^{-i(\omega t+\varphi_2)} \,. \tag{2.11}$$

The result needs to be real, so using the identity $e^{i\theta} = \cos\theta + i\sin\theta$ and then taking the real part produces

$$h(t) = B_1 \cos(\omega t + \varphi_1) + B_2 \cos(\omega t + \varphi_2) \,.$$

This can be rewritten as

$$h(t) = B_1 \cos(\omega t + \varphi_1) + B_2 \cos(\omega t + \varphi_1 - \varphi_3) \,.$$

Using the trigonometric identity $\cos(u - v) = \cos u \cos v + \sin u \sin v$ allows this to be written in the form

$$h(t) = B_1 \cos(\omega t + \varphi_1) + B_2 \Big(\cos(\omega t + \varphi_1)\cos(\varphi_3) + \sin(\omega t + \varphi_1)\sin(\varphi_3) \Big) \,.$$

Grouping the terms together and rewriting the constants gives

$$h(t) = B_3 \cos(\omega t + \varphi_1) + B_4 \sin(\omega t + \varphi_1) \,.$$

The constants can again be restated as

$$h(t) = B_5 \Big(b_1 \cos(\omega t + \varphi_1) + b_2 \sin(\omega t + \varphi_1) \Big) \,, \qquad \text{where} \quad b_1^2 + b_2^2 = 1 \,.$$

Knowing that $\cos^2\theta + \sin^2\theta = 1$, this allows $h(t)$ to be given in the form

$$h(t) = B_5 \Big(\sin(\varphi_4)\cos(\omega t + \varphi_1) + \cos(\varphi_4)\sin(\omega t + \varphi_1) \Big) \,.$$

Using the trigonometric identity $\sin(u + v) = \sin u \cos v + \cos u \sin v$, this can then be rewritten

$$h(t) = B_5 \sin(\omega t + \varphi_1 + \varphi_4) \,,$$

which then can finally be written as

$$\boxed{h(t) = B \sin(\omega t + \varphi) \,.} \tag{2.12}$$

This now gives the equation for z as $z(r, \theta, t) = f(r)\, g(r)\, B \sin(\omega t + \varphi)$. The next variable to solve is θ.

The $\frac{h_{tt}(t)}{h(t)}$ equality is discarded and the last two equalities from equation (2.8) are rearranged to give

$$c^2 \left(\frac{f_{rr}(r)}{f(r)} + \frac{1}{r}\frac{f_r(r)}{f(r)} \right) + \omega^2 = -\frac{c^2}{r^2}\frac{g_{\theta\theta}(\theta)}{g(\theta)} \,.$$

If both sides are multiplied by $\frac{r^2}{c^2}$ then the resulting equation is

$$r^2 \frac{f_{rr}(r)}{f(r)} + r\frac{f_r(r)}{f(r)} + \frac{\omega^2 r^2}{c^2} = -\frac{g_{\theta\theta}(\theta)}{g(\theta)} \,. \tag{2.13}$$

Now with independent variables on separate sides of the equation, both sides can again be set equal to a constant, this time called k_2 :

$$r^2\frac{f_{rr}(r)}{f(r)} + r\frac{f_r(r)}{f(r)} + \frac{\omega^2 r^2}{c^2} = -\frac{g_{\theta\theta}(\theta)}{g(\theta)} = k_2\,. \tag{2.14}$$

This gives an equation for $g(\theta)$ that is identical to the equation (2.9) for $h(t)$:

$$g_{\theta\theta}(\theta) = -k_2 g(\theta)\,.$$

This can be be solved in the same manner as equation (2.9) using the 2π periodicity of θ instead of the requirement of oscillations. This method produces the equation for $g(\theta)$, giving

$$\boxed{g(\theta) = C\sin(n\theta + \phi)\,,} \tag{2.15}$$

where $n = \sqrt{k_2} \in \mathbb{Z}$. To satisfy the 2π periodicity (the 3^{rd} boundary condition, equation (2.4)) n must be an integer.

The equation from (2.14) that is now left to solve is

$$r^2\frac{f_{rr}(r)}{f(r)} + r\frac{f_r(r)}{f(r)} + \frac{\omega^2 r^2}{c^2} = n^2\,.$$

This is multiplied by $f(r)$ and rearranged as

$$r^2 f_{rr}(r) + r f_r(r) + \left(\frac{\omega^2}{c^2}r^2 - n^2\right) f(r) = 0\,. \tag{2.16}$$

The solution to this is given in Appendix 1 as equation (A.9), and is a linear combination of $J_n\left(\frac{\omega r}{c}\right)$ and $Y_n\left(\frac{\omega r}{c}\right)$. However, $Y_n\left(\frac{\omega r}{c}\right)$ will tend to infinity as r tends to zero. This produces a singularity at $r = 0$, which contradicts the boundary condition given by equation (2.2). Therefore this part of the general solution is discarded. The z dependence on r is now written

$$\boxed{f(r) = D_n J_n\left(\frac{\omega r}{c}\right).} \tag{2.17}$$

It is noted that the amplitude D_n depends on the order n of the Bessel function. Combining all the components (2.12), (2.15) and (2.17) gives the solution to the original wave equation (2.1) :

$$z = A_n J_n\left(\frac{\omega r}{c}\right)\sin(\omega t + \varphi)\sin(n\theta + \phi)\,, \tag{2.18}$$

where $A_n = B\,C\,D_n$ and is the amplitude of the vibration for the particular mode of vibration.

Equation (2.18) describes the displacement for the mode of vibration at each position on the drum membrane for the allowed frequencies. To find the permitted frequencies the final boundary condition, equation (2.3) , is used. If this condition is used in equation (2.18) , the following equation is obtained:

$$J_n\left(\frac{\omega a}{c}\right) = 0\,. \tag{2.19}$$

Taking a and c as constants, the substitution can be made that $x = \lambda a = \frac{\omega}{c}a$. As a and c are constant the ratios of the different values of x are equal to the ratios of the different ω values. The equation then simply becomes the Bessel function set equal to zero:

$$\boxed{J_n(x_{nj}) = 0\,.} \tag{2.20}$$

When the equation is solved it will give the allowed ratios of the different frequencies of the drum, ie. the eigenfrequencies. If equation (2.18) is written without time-dependence then it becomes

$$\boxed{\psi_{nj} = A_{nj} J_n(\lambda_{nj} r)\sin(n\theta + \phi)\,,} \tag{2.21}$$

where λ_{nj} is restricted by the solutions of equation (2.20).

2.2 Frequencies of Vibration

Equation (2.20) is solved using Maple 12 software and the different solutions are labelled in the following way. The root is denoted x_{nj}, where the indices refer to the particular solution. n is identical to the n from the above equations and indicates the order of the Bessel function. j refers to the root number of this solution subset. The first root greater than 0 for the given n is labelled $j = 1$, the second root is labelled $j = 2$, and so on. To show more clearly the frequency ratios of the harmonics, every root is divided by the x_{01} root (the solution relating to the fundamental frequency), hence defining the x_{01} root as equal to 1. To comply with later notation and the notation of existing literature, the relative frequency of the x_{nj} root will be listed as the relative frequency of the ψ_{nj} mode of vibration.

The vibrational modes with a frequency up to 5.5 times the fundamental frequency are listed in the following table (Table 2.1). The work by Raman, described in the introduction, found the harmonics of the tabla above the fifth harmonic of insignificant amplitude due to damping effects. Although this damping is not present on the ordinary drum, this is the harmonic chosen as the last entry of this table. This is, in part, due to the purpose of this table being a comparison with the equivalent tables for the tabla models but also, as there are infinitely many solutions, a place to stop needs to be chosen at some point.

Note that the ψ_{02} root is incorrrectly listed as having a frequency ratio of 2.40 in both the Ramakrishna and Sondhi paper [RS] and the recent Gaudet et al. paper [GGL]. This result has been double checked.

The graphs of these modes of vibration are shown in Section 4.1 .

Mode	Frequency ratio	Mode	Frequency ratio
ψ_{01}	1.000	ψ_{51}	3.647
ψ_{11}	1.593	ψ_{32}	4.056
ψ_{21}	2.136	ψ_{61}	4.132
ψ_{02}	2.295	ψ_{13}	4.230
ψ_{31}	2.653	ψ_{42}	4.601
ψ_{12}	2.917	ψ_{23}	4.832
ψ_{41}	3.155	ψ_{04}	4.903
ψ_{22}	3.500	ψ_{52}	5.131
ψ_{03}	3.598	ψ_{33}	5.412

Table 2.1: Relative frequencies of the vibrational modes of the 1-density drum membrane

Chapter 3

The 2-Density Model

The model used here was first layed out in Ramakrishna and Sondhi's 1954 paper, 'Vibrations of Indian Musical Drums Regarded as Composite Membranes' [RS]. It models the right-handed tabla which is approximated to a drum membrane that has two regions of different density; the density of each region is constant. The syahi of the tabla is not of constant density so this model will not fully reproduce the vibrations of the tabla. This model also does not account for the effect of air pressure within the shell of the drum.

3.1 Solving the Wave Equation for the 2-Density Model

The radius of the inner region of the drum is a and the radius of the outer region is b (see Figure 3.1). The right-handed drum will be solved here and the inner section $(0 \leq r \leq a)$ shall have a density $\rho = \rho_1$, and the outer section $(a \leq r \leq b)$ a density $\rho = \rho_2$.

As in the 1-density case, the solution of the wave equation, extended to two dimensions, is required for a model of the drum:

$$\frac{\partial^2 z}{\partial t^2} = c^2 \nabla^2 z \,. \tag{3.1}$$

The method for solving the wave equation is again by separation of variables, and to separate the variable t, z can be written in the form $z(r, \theta, t) = \psi(r, \theta)h(t)$, allowing the wave equation to be written as

$$\psi(r, \theta)h(t)_{tt} = c^2 h(t) \nabla^2 \psi(r, \theta) \,. \tag{3.2}$$

The equation is divided by $z(r, \theta, t)$. This produces independent variables on each side and allows both sides of the equation to be set equal to the constant $-\omega^2$. The equation then becomes

$$\frac{h_{tt}}{h} = c^2 \frac{\nabla^2 \psi}{\psi} = -\omega^2 \,. \tag{3.3}$$

The same method used in the 1-density case solves the function $h(t)$ and again gives $h(t) = B\sin(\omega t + \phi)$. The wave equation is now time-independent and written using the function of $\psi(r, \theta)$. It is rearranged to give

$$\nabla^2 \psi + \frac{\omega^2}{c^2}\psi = 0 \,, \tag{3.4}$$

where, as before, $c^2 = \frac{T}{\rho}$. The value of c is different for the different regions of the drum as the density differs. The tension is uniform across both regions because the loading is applied to the surface of the membrane. These different values define λ_i as

$$\lambda_1 = \frac{\omega}{c_1} = \omega\sqrt{\frac{\rho_1}{T}} \qquad \text{when} \qquad 0 \leq r \leq a \,,$$
$$\lambda_2 = \frac{\omega}{c_2} = \omega\sqrt{\frac{\rho_2}{T}} \qquad \text{when} \qquad a \leq r \leq b \,.$$

Two different equations are now written for the two differents regions of the drum:

$$\nabla^2 \psi_1 + \lambda_1^2 \psi_1 = 0 \quad 0 \leq r \leq a \,, \tag{3.5}$$

$$\nabla^2 \psi_2 + \lambda_2^2 \psi_2 = 0 \quad a \leq r \leq b \,. \tag{3.6}$$

The regions and their densities are shown in Figure 3.1 .

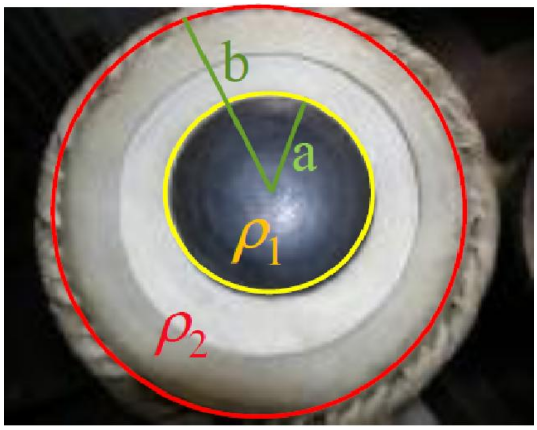

Figure 3.1: The regions of the 2 density model[4]

Next boundary conditions are imposed on the equations. The edge of the membrane is fixed, so the displacement must equal zero at the edge of the drum. Also, where the inner and outer sections of the membrane meet the function ψ and its gradient must be equal for both regions. As the tension is constant for both sections the gradients are not

[4]Image from http://bobbysingh.com.au and edited using Microsoft Powerpoint

stress-weighted. Additionally the function is 2π periodic and must be constant within the region of the drum, giving the boundary conditions:

$$\psi(r,\theta) \in \mathbb{R} \quad \text{when} \quad 0 \leq r \leq b\,, \tag{3.7}$$
$$\psi_2(b,\theta) = 0\,, \tag{3.8}$$
$$\psi_1(a,\theta) = \psi_2(a,\theta)\,, \tag{3.9}$$
$$\frac{\partial}{\partial r}\psi_1(a,\theta) = \frac{\partial}{\partial r}\psi_2(a,\theta)\,, \tag{3.10}$$
$$\psi_i(r,\theta) = \psi_i(r,\theta + 2\pi n)\,. \tag{3.11}$$

The equations (3.5) and (3.6) can then be solved in the same manner as the ordinary drum but, unlike the normal drum, the solution to ψ_2 must include the Bessel function of the second kind because ψ_2 does not exist at $r = 0$, so will not produce a singularity there. This gives the solutions

$$\psi_1(r,\theta) = A_n J_n(\lambda_1 r)\sin(n\theta + \phi_n)\,, \tag{3.12}$$
$$\psi_2(r,\theta) = [B_n J_n(\lambda_2 r) + C_n Y_n(\lambda_2 r)]\sin(n\theta + \phi_n)\,. \tag{3.13}$$

These equations must be altered so that they have equal displacement and gradient where they meet. The frequencies of the vibrational modes can then be determined by solving the equation at the edge of the drum.

If the solutions to the wave equation for the different regions (3.12 and 3.13) are entered into the boundary conditions (3.8) and (3.9) they become:

$$B_n J_n(\lambda_2 b) + C_n Y_n(\lambda_2 b) = 0\,, \tag{3.14}$$
$$A_n J_n(\lambda_1 a) = B_n J_n(\lambda_2 a) + C_n Y_n(\lambda_2 a)\,. \tag{3.15}$$

Entered into equation (3.10) the two halves of the equation for the gradient are:

$$\frac{\partial}{\partial r}\psi_1(a,\theta) = \lambda_1\left(-\frac{n}{\lambda_1 a}A_n J_n(\lambda_1 a)\sin(n\theta+\phi_n) + A_n J_{n-1}(\lambda_1 a)\sin(n\theta+\phi_n)\right)\,, \tag{3.16}$$

$$\begin{aligned}\frac{\partial}{\partial r}\psi_2(a,\theta) = \lambda_2\Bigg(&-\frac{n}{\lambda_2 a}B_n J_n(\lambda_2 a)\sin(n\theta+\phi_n) + B_n J_{n-1}(\lambda_2 a)\sin(n\theta+\phi_n)\\ &-\frac{n}{\lambda_2 a}C_n Y_n(\lambda_2 a)\sin(n\theta+\phi_n) + C_n Y_{n-1}(\lambda_2 a)\sin(n\theta+\phi_n)\Bigg)\,.\end{aligned} \tag{3.17}$$

These two are set equal to one another to satisfy (3.10). The $\sin(n\theta + \phi_n)$ term cancels

out to give

$$\lambda_1\left(-\frac{n}{\lambda_1 a}A_nJ_n(\lambda_1 a)+A_nJ_{n-1}(\lambda_1 a)\right)=\lambda_2\left(-\frac{n}{\lambda_2 a}B_nJ_n(\lambda_2 a)+B_nJ_{n-1}(\lambda_2 a)\right.$$
$$\left.-\frac{n}{\lambda_2 a}C_nY_n(\lambda_2 a)+C_nY_{n-1}(\lambda_2 a)\right). \tag{3.18}$$

The next stage is to find an equation which is independent of all the coefficients so that it can be solved to find the allowed frequency ratios. First (3.18) is divided by (3.15), which cancels A_n out and now leaves the equation independent of one of the coefficients. This equation is

$$\frac{\lambda_1}{\lambda_2}\frac{J_{n-1}(\lambda_1 a)}{J_n(\lambda_1 a)}=\frac{B_nJ_{n-1}(\lambda_2 a)+C_nY_{n-1}(\lambda_2 a)}{B_nJ_n(\lambda_2 a)+C_nY_n(\lambda_2 a)}. \tag{3.19}$$

Dividing both the numerator and denominator of the right hand side by C_n produces

$$\frac{\lambda_1}{\lambda_2}\frac{J_{n-1}(\lambda_1 a)}{J_n(\lambda_1 a)}=\frac{\frac{B_n}{C_n}J_{n-1}(\lambda_2 a)+Y_{n-1}(\lambda_2 a)}{\frac{B_n}{C_n}J_n(\lambda_2 a)+Y_n(\lambda_2 a)}. \tag{3.20}$$

To eliminate B_n and C_n from this equation, equation (3.14) is rearranged to the form $\frac{B_n}{C_n}=-\frac{Y_n(\lambda_2 b)}{J_n(\lambda_2 b)}$, which is the substituted in for $\frac{B_n}{C_n}$. The equation becomes

$$\frac{\lambda_1}{\lambda_2}\frac{J_{n-1}(\lambda_1 a)}{J_n(\lambda_1 a)}=\frac{-\frac{Y_n(\lambda_2 b)}{J_n(\lambda_2 b)}J_{n-1}(\lambda_2 a)+Y_{n-1}(\lambda_2 a)}{-\frac{Y_n(\lambda_2 b)}{J_n(\lambda_2 b)}J_n(\lambda_2 a)+Y_n(\lambda_2 a)}. \tag{3.21}$$

Rearranging this by multiplying the right by $\frac{-J_n(\lambda_2 b)}{-J_n(\lambda_2 b}$ produces

$$\frac{\lambda_1}{\lambda_2}\frac{J_{n-1}(\lambda_1 a)}{J_n(\lambda_1 a)}=\frac{Y_n(\lambda_2 b)J_{n-1}(\lambda_2 a)-J_n(\lambda_2 b)Y_{n-1}(\lambda_2 a)}{Y_n(\lambda_2 b)J_n(\lambda_2 a)-J_n(\lambda_2 b)Y_n(\lambda_2 a)}. \tag{3.22}$$

There is now a change to one variable that depends on the frequency, for which the equation can be solved. The quantities are defined as

$$x=\lambda_2 b=\frac{\omega b}{c_2},$$
$$\sigma^2=\frac{\rho_1}{\rho_2}=\frac{\lambda_1^2}{\lambda_2^2},$$
$$k=\frac{a}{b}.$$

It is noted that $\sigma^2=\frac{\lambda_1^2}{\lambda_2^2}$ is a fixed ratio equal to the ratio of densities and k is a fixed ratio equal to the ratio of radii.

The new quantities are now subsituted into (3.22) and this gives an equation that can be numerically solved for x with a given σ^2 and k. This is the equation whose solutions are the frequency eigenvalues:

$$\boxed{\sigma \frac{J_{n-1}(\sigma k x)}{J_n(\sigma k x)} = \frac{Y_n(x)J_{n-1}(kx) - J_n(x)Y_{n-1}(kx)}{Y_n(x)J_n(kx) - J_n(x)Y_n(kx)}\,.} \tag{3.23}$$

It is noted that this equation is undefined when $k = 1$ but the 1-density case can still be solved by using $\sigma = 1$. When equation (3.23) is solved for x it will provide the permitted relative frequencies of the modes of vibration. Provided the values for b (the radius of the whole membrane) and c_2, which can be calculated from the equation $c = \sqrt{\frac{T}{\rho_2}}$, are known the frequency of the vibration can be found. Alternatively, knowing the values of b and ρ_2 and the desired frequency, the solution can tell the tabla player the tension to tighten the drum to to achieve that frequency.

There will be more than one solution to this equation for a given n, σ and k, so the jth root of equation (3.23) will be denoted x_{nj}.

To get the equations of displacement of the two regions for each distinct x_{nj} there will be different ratios of A_{nj}, B_{nj} and C_{nj}. Just one coefficient is wanted, A_{nj}, which will be the amplitude of the system. To obtain B_{nj} in terms of A_{nj} the equation (3.14), $C_{nj} = -\frac{B_{nj}J_n(x_{nj})}{Y_n(x_{nj})}$, is substituted into equation (3.15), getting

$$A_{nj}J_n(\sigma k x_{nj}) = B_{nj}J_n(kx_{nj}) - \frac{B_{nj}J_n(x_{nj})}{Y_n(x_{nj})}Y_n(kx_{nj})\,. \tag{3.24}$$

Rearranging to make B_{nj} the subject, this becomes

$$B_{nj} = A_{nj}\frac{J_n(\sigma k x_{nj})Y_n(x_{nj})}{J_n(kx_{nj})Y_n(x_{nj}) - J_n(x_{nj})Y_n(kx_{nj})}\,. \tag{3.25}$$

Similarly substituting from equation (3.14) $B_{nj} = -\frac{C_{nj}Y_n(x_{nj})}{J_n(x_{nj})}$ into equation (3.15), gives C_{nj} as

$$C_{nj} = -A_{nj}\frac{J_n(\sigma k x_{nj})J_n(x_{nj})}{J_n(kx_{nj})Y_n(x_{nj}) - J_n(x_{nj})Y_n(kx_{nj})}\,. \tag{3.26}$$

The solutions of ψ for the two different regions are now

$$\psi_{1nj}(r,\theta) = A_{nj}J_n\left(\frac{\sigma k x_{nj}}{a}\,r\right)\sin(n\theta + \phi_n)\,, \tag{3.27}$$

$$\begin{aligned}\psi_{2nj}(r,\theta) = A_{nj}&\frac{J_n(\sigma k x_{nj})}{J_n(kx_{nj})Y_n(x_{nj}) - J_n(x_{nj})Y_n(kx_{nj})}\\ &\times\left[Y_n(x_{nj})J_n\left(\frac{x_{nj}}{b}\,r\right) - J_n(x_{nj})Y_n\left(\frac{x_{nj}}{b}\,r\right)\right]\sin(n\theta + \phi_n)\,.\end{aligned} \tag{3.28}$$

3.2 Tuning the 2-Density Drum

The harmonics frequencies of the tabla that are relevant to the 2-density model are the relative frequencies of the open wooden shell from Table 1.1. The model doesn't take into account the air pressure, so the values for the tabla in normal use are not as applicable to this model. The frequencies for the open shell tabla are very close to perfect harmonicity so Ramakrishna and Sondhi, whose values depart much further from perfect harmonicity than the real world values, chose to tune their membrane towards perfect harmonicity rather than the observed values of tabla. This is the goal towards which tabla-makers have evolved the tabla and it is assumed that this would be the tabla-maker's ideal for their constructed tabla. The 2-density model also has errors greater than the error between perfect harmonicity and the experimental values. The approach of [RS] is therefore the approach taken here, with the error calculated as departing from the perfect harmonics rather than the observed frequencies.

3.2.1 Optimizing σ and k

There now exists a set of solutions to the eigenvalue equation that are denoted x_{nj}. Each solution is related to the frequency by the equation

$$x_{nj} = 2\pi f\, b \sqrt{\frac{\rho_2}{T}}\,. \tag{3.29}$$

b, ρ_2 and T are constants so there is a linear relationship between x_{nj} and the frequency. For the drum to be perfectly in tune all the harmonics have to be integer ratios of the fundamental frequency ie. $\frac{x_{nj}}{x_{01}} = 1, 2, 3\ldots$.

To get different solutions of x_{nj}, σ and k can be varied and as this is done the proximity of the $\frac{x_{nj}}{x_{01}}$ values to the integers changes. The harmonic error is a calculation of how far the harmonics are from the integer multiples. The error shall be calculated from the error defined by Gaudet et al. [GGL]. This weights the lower harmonics to mirror the increased amplitude of these harmonics in the tabla and is given by

$$\text{Error} = \sum_{h=2}^{5} \sum_{d=1}^{D} \left(\frac{\frac{x_{nj}}{x_{01}} - h}{h} \right)^2 , \tag{3.30}$$

where h is the integer value of the harmonic that $\frac{x_{nj}}{x_{01}}$ is closest to and D is the number of degenerate modes. Harmonics $h \geq 6$ are ignored due to the damping effect of the outer halo. This error equation was not used by Ramakrishna and Sondhi who set $k = 0.4$ and arrived at their value for σ by graphical methods.

Starting with the values given by Ramakrishna and Sondhi [RS], Maple 12 is used to vary σ and k to 3 significant figures until the minimum error was reached (program C.2). This optimizes σ and k to produce the lowest harmonic error within the model, assuming there isn't a local minimum between the [RS] values and the global minimum. It is recognised that in practice it would be very difficult for tabla makers to achieve the three significant figure level of precision using their construction techniques for the tabla (changing k by

the third significant figure is a change of approximately 0.1mm). This level of precision is included as it can still affect the harmonic ratios so that the frequency changes are within the limit of the human ear ($\approx$ 4Hz).

ψ_{nj} represents the modes of vibration relating to $\frac{x_{nj}}{x_{01}}$. The optimal values in this case were found to be $\sigma = 3.15$ and $k = 0.401$, with an error of 0.0044226 produced. The values of σ and k found by [RS] for real-world tablas are

$$3 < \sigma < 4\,, \tag{3.31}$$

$$0.45 < k < 0.55\,, \tag{3.32}$$

meaning this value of k lies well outside the range. For a completely accurate model of the right-handed tabla, the value of k must fall within this range. A comparison of the frequencies of the different vibrational modes for the above values of k and σ are shown in Table 3.1 .

	Frequency ratio	
Mode	Rama. and Sondhi $\sigma = 3.125$ $k = 0.4$	Maple 12 optimization $\sigma = 3.15$ $k = 0.401$
ψ_{01}	1.00	1.00
ψ_{11}	1.94	1.94
ψ_{21}	2.95	2.94
ψ_{02}	3.05	3.05
ψ_{31}	3.97	3.96
ψ_{12}	4.10	4.10
ψ_{03}	4.82	4.84
ψ_{41}	4.97	4.96
ψ_{22}	5.14	5.16
Error	0.0044500	0.0044226

Table 3.1: Comparison of frequency ratios of harmonics by varying σ and k, with ψ_{03} as the 5^{th} harmonic

From Table 3.1 it can be seen that the 2-density model has good agreement with perfect harmonicity. As the tabla is approximately harmonic the model also has good agreement with the tabla.

Gaudet, Gauthier and Léger [GGL] found that if ψ_{03} was set to be the 6^{th} rather than 5^{th} harmonic then the error was significantly reduced. They also include the ψ_{13} harmonic as part of their analysis as it then falls close to the 5^{th} harmonic.

This departs even further from the real-world than the idealized membrane used by Ramakrishna and Sondhi. If the model is trying only to emulate the real-world tabla then this could not be used as a technique for lowering the error as the ψ_{03} harmonic has been experimentally found to fall close to the 5^{th} harmonic. The significant lowering of the error by this change raises interesting questions about the evolution of the drum. The drum must have evolved through a stage similar to the two-density model and better harmonicity at this stage would be achieved by a 6^{th} harmonic for the ψ_{03} model.

Again σ and k have been varied to 3 significant figures. The optimal values in this case

were found to be $\sigma = 2.84$ and $k = 0.385$, with an error of 0.0018872 produced. The frequency eigenvalues for this result are shown in Table 3.2. With the placing of ψ_{03} at the 6^{th} harmonic the values for both σ and k depart further from their experimental values.

	Frequency ratio	
Mode	Gaud., Gauth. and Léger $\sigma = 2.9$ $k = 0.38$	Maple 12 Optimization $\sigma = 2.84$ $k = 0.385$
ψ_{01}	1.00	1.00
ψ_{11}	1.96	1.95
ψ_{21}	3.00	2.98
ψ_{02}	3.05	3.04
ψ_{12}	4.02	3.99
ψ_{31}	4.05	4.03
ψ_{22}	4.95	4.91
ψ_{41}	5.09	5.06
ψ_{13}	5.14	5.12
ψ_{03}*	5.99	5.96
Error	0.0021392	0.0018872

Table 3.2: Comparison of frequency ratios of harmonics by varying σ and k, with ψ_{03} as the 6^{th} harmonic, therefore not included in error calculation

The difference between the errors of placing ψ_{03} at the two different harmonics shows the greatly superior harmonicity of the ψ_{03} frequency when near the 6^{th} harmonic. This shows that for the idealized 2-density membrane greater harmonicity can be achieved with a model that departs from the tabla.

Using the values of $\sigma = 3.15$ and $k = 0.401$ the tension in the membrane required to produce a certain frequency can be found. The fundamental frequency $x_{01} = 0.998$ is used in the equation. Rearranging equation (3.29) gives

$$T = 4\pi^2 f^2 \frac{b^2 \rho_2}{x_{01}^2} \tag{3.33}$$

A typical diameter and pitch of the right-handed tabla are 5.5" (radius of b=0.06985 m)[1] and F_3 ($f = 174.6$ Hz) is used. Using equation (3.33) and the density (0.24 kg m^{-2}), which was given for a synthetic drum membrane by Howle and Trefethen [HT], equates to a required tension of 1415 $N\,m^{-1}$. As the density of the tabla membrane is likely to be greater than a synthetic drum membrane and the tightening mechanisms aren't as powerful this appears reasonable when compared to their value of tension for a kettledrum: T=4415 $N\,m^{-1}$.

[1] kksongs.org/tabla/chapter34.html

Chapter 4

Modes of Vibration of the Drums and a Comparison of the Models

The solutions to two different drums have now been calculated and, from these solutions, graphs showing their vibrational characteristics can be created. A comparison between the eigenfrequency ratios and the harmonicity of the drums can also be made.

4.1 Graphs of the Vibrational Modes

Using the displacement equation (2.21) for the 1-density drum and equations (3.27) and (3.28) for the 2-density model with $\sigma = 3.14$ and $k = 0.401$, a time-independent graph for each mode of vibration can be drawn. These graphs show the displacement at maximum amplitude and are rotated to provide the best view rather than having a particular orientation for θ. The graphs can be thought of as the actual membrane of the drum with an exaggerated displacement. The edge of the graph represents the edge of the drum and the surface of the graph represents the membrane of the drum at a moment in time.

The values of n and j are physically evident as n is equal to the number of diameter lines that have a time-independent displacement of zero and j is equal to the number of circles of constant r, including the edge of the drum, that have a time-independent displacement of zero. The central high density region causes the 2-density model to have a different profile of vibration than the 1-density drum. The graphs are notably different even though the same restrictions due to n and j apply. The graphs are plotted by Maple 12 (using program C.1).

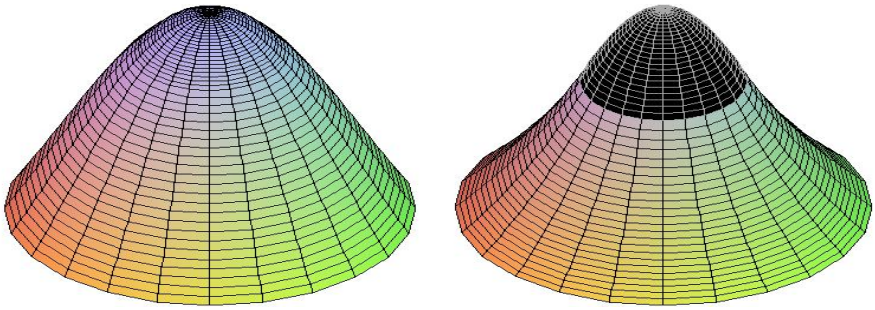

(a) 1-density (b) 2-density

Figure 4.1: $\psi_{01}(r, \theta)$ for one-density and two-density concentric drum

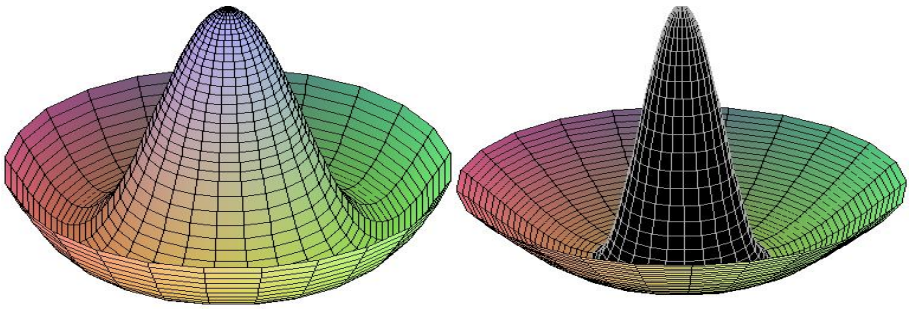

(a) 1-density (b) 2-density

Figure 4.2: $\psi_{02}(r, \theta)$ for one-density and two-density concentric drum

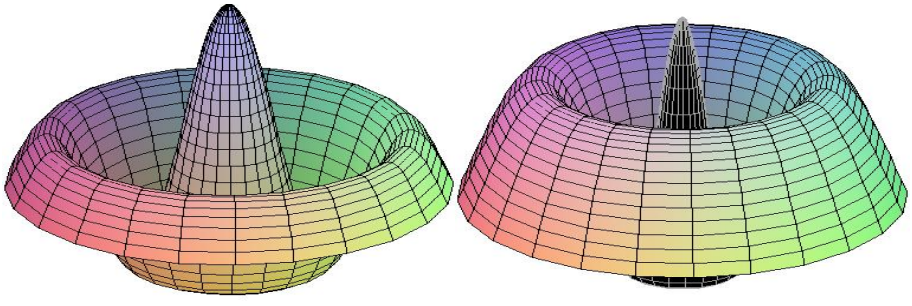

(a) 1-density (b) 2-density

Figure 4.3: $\psi_{03}(r, \theta)$ for one-density and two-density concentric drum

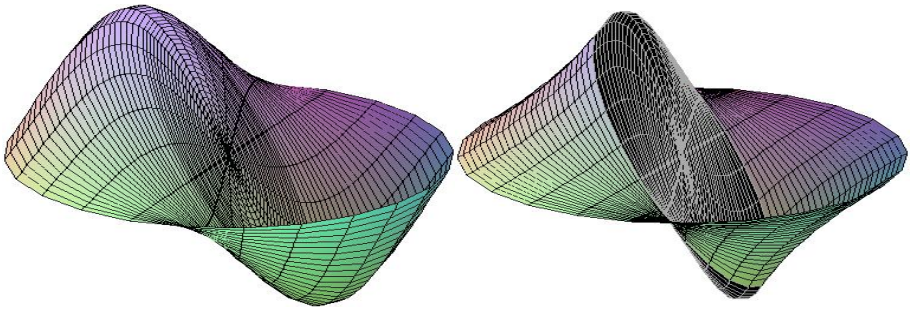

(a) 1-density (b) 2-density

Figure 4.4: $\psi_{11}(r, \theta)$ for one-density and two-density concentric drum

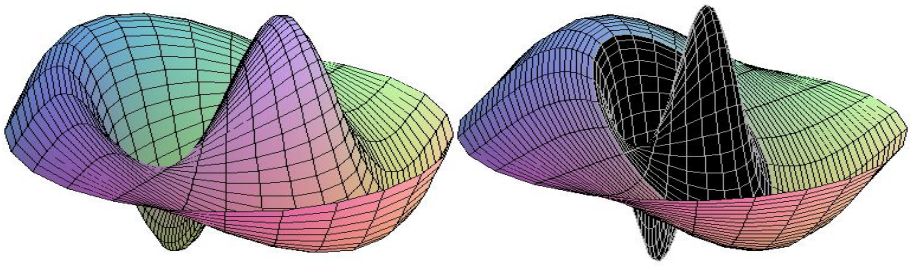

(a) 1-density (b) 2-density

Figure 4.5: $\psi_{12}(r, \theta)$ for one-density and two-density concentric drum

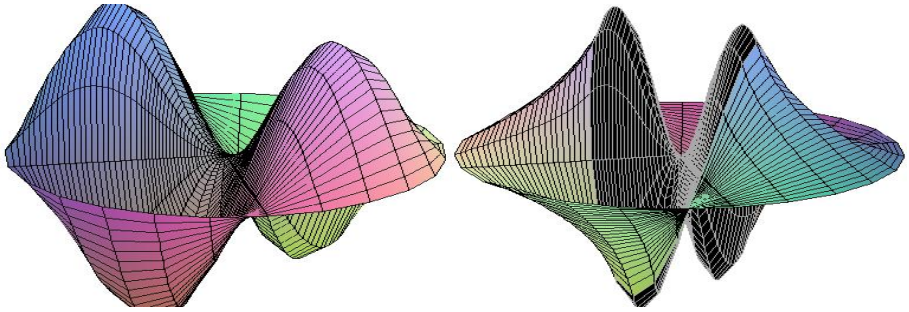

(a) 1-density (b) 2-density

Figure 4.6: $\psi_{21}(r, \theta)$ for one-density and two-density concentric drum

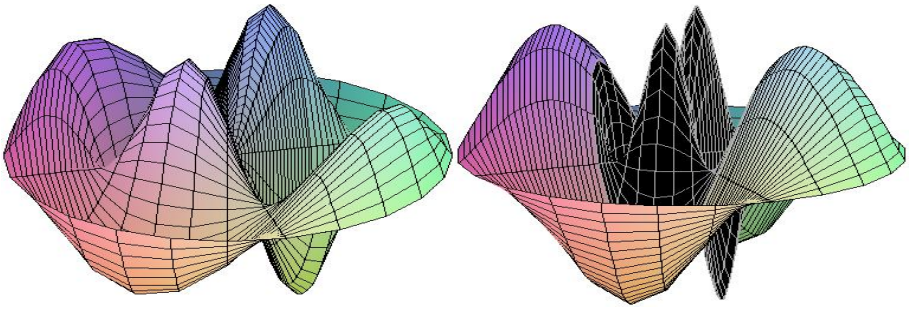

(a) 1-density (b) 2-density

Figure 4.7: $\psi_{22}(r, \theta)$ for one-density and two-density concentric drum

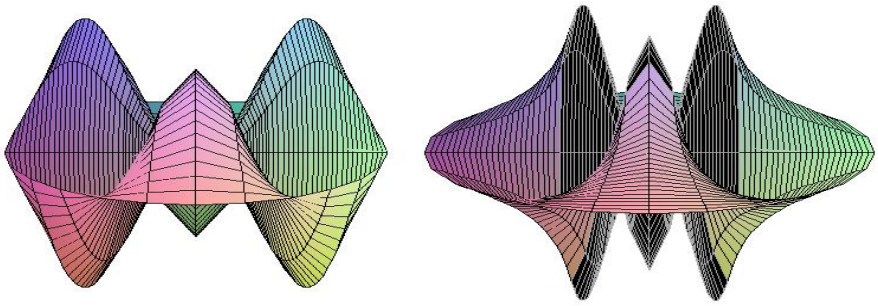

(a) 1-density (b) 2-density

Figure 4.8: $\psi_{31}(r, \theta)$ for one-density and two-density concentric drum

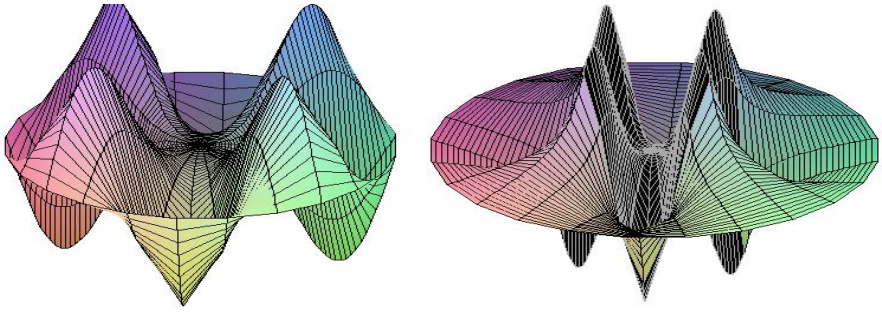

(a) 1-density (b) 2-density

Figure 4.9: $\psi_{41}(r, \theta)$ for one-density and two-density concentric drum

4.2 Comparison of Harmonicity

This section compares the eigenfrequencies from Tables 2.1 and 3.2 . The allowed frequencies of the ordinary drum bear no relation to the frequencies of the harmonics creating a completely inharmonic instrument. In contrast to this, if a constant region of higher density is added to the centre of the drum then a model with good levels of harmonicity can be created. In addition to the absense of any relation between the harmonics and the eigenfrequency ratios, the 1-density drum also has a much greater number of allowed frequencies between the fundamental frequency and the 5^{th} harmonic. These differences can clearly be seen in Figure 4.10 .

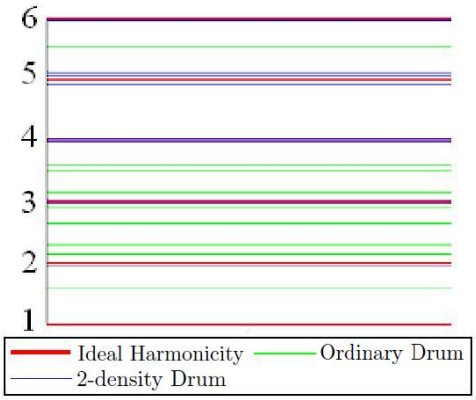

Figure 4.10: The relative frequencies of the harmonics belonging to the 1-density and 2-density models, compared with ideal harmonicity

From the enclosed CD it can be heard that these sets of harmonics create effects that are audibly very different from each other. The harmonics of the ordinary drum have no discernable tuning and as expected produce a sound that bears relation to a normal drum. The harmonics of the 2-density model produce a note that is audibly close to a harmonic note, although there is clearly a level of tuning error.

Chapter 5

The 3-Density Model

A 3-density model is a logical step to improve upon the harmonicity of the 2-density model . This also mirrors the construction of the tabla whose loaded portion has an increase in thickness towards its centre. After an abrupt change in radial density between the edge of the syahi and the outer membrane the differences are then less pronounced within the syahi. The 3-density model should better replicate the real-world tabla and reduce the harmonic error. The relative densities of the inner two regions are expected to be closer to equality than the relative densities of the outer two regions.

5.1 Solving the Wave Equation for the 3-Density Model

Using the same method as was used to solve the right-handed tabla, the wave equation of a drum with three different densities is now solved. The inner-most section ($0 \leq r \leq a$) shall have a density $\rho = \rho_1$, the middle section ($a \leq r \leq b$) shall have $\rho = \rho_2$ and the outer section ($b \leq r \leq l$) shall have a density $\rho = \rho_3$, l being the edge of the drum.

Again the two-dimensional wave equation is started with:

$$\frac{\partial^2 z}{\partial t^2} = c^2 \nabla^2 z \,. \tag{5.1}$$

As before, to use a separation of variables method $z(r, \theta, t)$ is written in the form $z(r, \theta, t) = \psi(r, \theta)h(t)$, allowing the wave equation to be written as

$$\psi(r, \theta)h(t)_{tt} = c^2 h(t) \nabla^2 \psi(r, \theta)) \,. \tag{5.2}$$

The equation is divided by $z(r, \theta, t) = \psi(r, \theta)h(t)$. This produces independent variables on each side and allows both sides of the equation to be set equal to the constant $-\omega^2$. The equation then becomes

$$\frac{h_{tt}}{h} = c^2 \frac{\nabla^2 \psi}{\psi} = -\omega^2 \,. \tag{5.3}$$

The solution to $h(t)$ is the same as the previous cases: $h(t) = \sin(\omega t + \varphi_n)$.

Rearranging the right two equivalences of equation (5.3) produces the time-independent equation

$$\nabla^2 \psi + \frac{\omega^2}{c^2} \psi = 0 \,, \tag{5.4}$$

where the value of $c^2 = \frac{T}{\rho}$. The next step is to define λ for each region of the drum.

$$\begin{aligned}
\lambda_1 &= \frac{\omega}{c_1} = \omega \sqrt{\frac{\rho_1}{T}} \qquad \text{when} \quad 0 \leq r \leq a \,, \\
\lambda_2 &= \frac{\omega}{c_2} = \omega \sqrt{\frac{\rho_2}{T}} \qquad \text{when} \quad a \leq r \leq b \,, \\
\lambda_3 &= \frac{\omega}{c_3} = \omega \sqrt{\frac{\rho_3}{T}} \qquad \text{when} \quad b \leq r \leq l \,.
\end{aligned}$$

Now the equations for each region of the drum can be written in the form

$$\nabla^2 \psi_1 + \lambda_1^2 \psi_1 = 0 \quad 0 \leq r \leq a \,, \tag{5.5}$$

$$\nabla^2 \psi_2 + \lambda_2^2 \psi_2 = 0 \quad a \leq r \leq b \,, \tag{5.6}$$

$$\nabla^3 \psi_3 + \lambda_3^2 \psi_3 = 0 \quad b \leq r \leq l \,. \tag{5.7}$$

These regions and their densities are shown in Figure 5.1 .

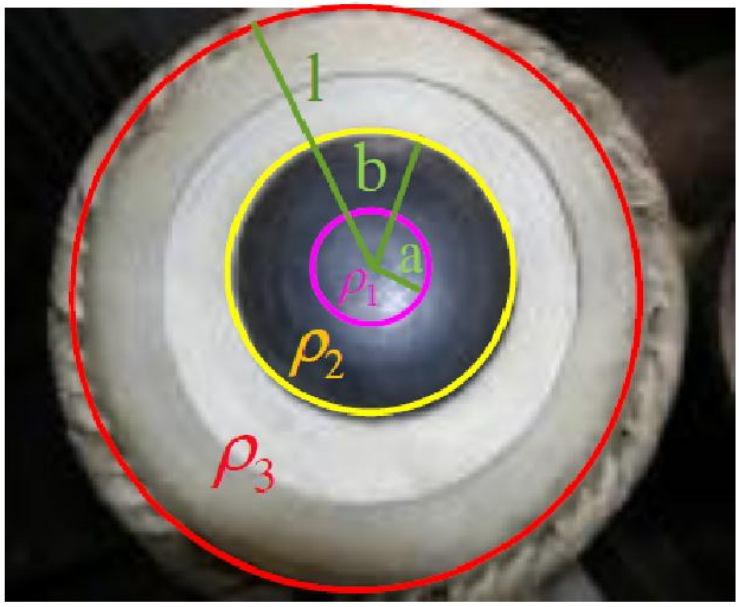

Figure 5.1: The regions of the 3 density model[5]

As before, the next step is to impose boundary conditions on the equations. The same boundary conditions as the 2-density model are used but with the addition of two more. There are now two different radii, a and b, where different sections of the membrane meet and at both of these the function ψ and its gradient must be equal in the adjacent regions.

$$\psi(r,\theta) \in \mathbb{R} \quad \text{when} \quad 0 \leq r \leq l\,, \tag{5.8}$$
$$\psi_3(l,\theta) = 0\,, \tag{5.9}$$
$$\psi_1(a,\theta) = \psi_2(a,\theta)\,, \tag{5.10}$$
$$\psi_2(b,\theta) = \psi_3(b,\theta)\,, \tag{5.11}$$
$$\frac{\partial}{\partial r}\psi_1(a,\theta) = \frac{\partial}{\partial r}\psi_2(a,\theta)\,, \tag{5.12}$$
$$\frac{\partial}{\partial r}\psi_2(b,\theta) = \frac{\partial}{\partial r}\psi_3(b,\theta)\,, \tag{5.13}$$
$$\psi(r,\theta) = \psi(r,\theta+2\pi n)\,. \tag{5.14}$$

Equations (5.5), (5.6) and (5.7) can then be solved in the same manner as the normal drum but, unlike the normal drum, the solutions to ψ_2 and now ψ_3 must include the Bessel function of the second kind because the domains of both ψ_2 and ψ_2 do not include $r = 0$, so will not produce a singularity. This property and the solution of the wave equation for each region gives the general solutions

$$\psi_1(r,\theta) = A_n J_n(\lambda_1 r)\sin(n\theta+\phi_n)\,, \tag{5.15}$$
$$\psi_2(r,\theta) = [B_n J_n(\lambda_2 r) + C_n Y_n(\lambda_2 r)]\sin(n\theta+\phi_n)\,, \tag{5.16}$$

[5]Image from http://bobbysingh.com.au and edited using Microsoft Powerpoint

$$\psi_3(r,\theta) = [D_n J_n(\lambda_3 r) + E_n Y_n(\lambda_3 r)]\sin(n\theta + \phi_n)\,. \tag{5.17}$$

If these results are entered into the boundary conditions (5.9), (5.10), (5.11), (5.12) and (5.13), then (5.9), (5.10) and (5.11) become

$$D_n J_n(\lambda_3 l) + E_n Y_n(\lambda_3 l) = 0\,, \tag{5.18}$$

$$A_n J_n(\lambda_1 a) = B_n J_n(\lambda_2 a) + C_n Y_n(\lambda_2 a)\,, \tag{5.19}$$

$$B_n J_n(\lambda_2 b) + C_n Y_n(\lambda_2 b) = D_n J_n(\lambda_3 b) + E_n Y_n(\lambda_3 b) \tag{5.20}$$

and the two sides of equation (5.12) become

$$\frac{\partial}{\partial r}\psi_1(a,\theta) = \lambda_1\left(-\frac{n}{\lambda_1 a}A_n J_n(\lambda_1 a)\sin(n\theta+\phi_n) + A_n J_{n-1}(\lambda_1 a)\sin(n\theta+\phi_n)\right), \tag{5.21}$$

$$\begin{aligned}\frac{\partial}{\partial r}\psi_2(a,\theta) = \lambda_2\Bigg(&-\frac{n}{\lambda_2 a}\,B_n J_n(\lambda_2 a)\sin(n\theta+\phi_n) + B_n J_{n-1}(\lambda_2 a)\sin(n\theta+\phi_n)\\ &-\frac{n}{\lambda_2 a}C_n Y_n(\lambda_2 a)\sin(n\theta+\phi_n) + C_n Y_{n-1}(\lambda_2 a)\sin(n\theta+\phi_n)\Bigg).\end{aligned} \tag{5.22}$$

These two are put equal to one another to satisfy (5.12), with $\sin(n\theta+\phi_n)$ cancelling:

$$\begin{aligned}\lambda_1\left(-\frac{n}{\lambda_1 a}A_n J_n(\lambda_1 a) + A_n J_{n-1}(\lambda_1 a)\right) = \lambda_2\Bigg(&-\frac{n}{\lambda_2 a}B_n J_n(\lambda_2 a) + B_n J_{n-1}(\lambda_2 a)\\ &-\frac{n}{\lambda_2 a}C_n Y_n(\lambda_2 a) + C_n Y_{n-1}(\lambda_2 a)\Bigg)\,.\end{aligned} \tag{5.23}$$

Similarly, differentiating ψ_2 and ψ_3 and setting them equal to each other at b the boundary condition (5.13) is observed producing

$$\begin{aligned}&\lambda_2\left(-\frac{n}{\lambda_2 b}B_n J_n(\lambda_2 b) + B_n J_{n-1}(\lambda_2 b) - \frac{n}{\lambda_2 b}C_n Y_n(\lambda_2 b) + C_n Y_{n-1}(\lambda_2 b)\right) =\\ &\lambda_3\left(-\frac{n}{\lambda_3 b}D_n J_n(\lambda_3 b) + D_n J_{n-1}(\lambda_3 b) - \frac{n}{\lambda_3 b}E_n Y_n(\lambda_3 b) + E_n Y_{n-1}(\lambda_3 b)\right).\end{aligned} \tag{5.24}$$

The next step is find an equation which is independent of all the coefficients which will provide the frequency eigenvalues when solved. First $\frac{B_n}{C_n}$ and $\frac{D_n}{E_n}$ are needed in a form independent of the coefficients. Rearranging (5.18) gives

$$\frac{D_n}{E_n} = -\frac{Y_n(\lambda_3 l)}{J_n(\lambda_3 l)}\,. \tag{5.25}$$

To get $\frac{B_n}{C_n}$ equation (5.23) is divided by (5.19)

$$\frac{\lambda_1}{\lambda_2}\frac{J_{n-1}(\lambda_1 a)}{J_n(\lambda_1 a)} = \frac{B_n J_{n-1}(\lambda_2 a) + C_n Y_{n-1}(\lambda_2 a)}{B_n J_n(\lambda_2 a) + C_n Y_n(\lambda_2 a)}\,. \tag{5.26}$$

Dividing both the numerator and denominator of the right-hand side by C_n produces

$$\frac{\lambda_1}{\lambda_2}\frac{J_{n-1}(\lambda_1 a)}{J_n(\lambda_1 a)} = \frac{\frac{B_n}{C_n}J_{n-1}(\lambda_2 a) + Y_{n-1}(\lambda_2 a)}{\frac{B_n}{C_n}J_n(\lambda_2 a) + Y_n(\lambda_2 a)}\,. \tag{5.27}$$

Rearranging this produces the equation

$$\frac{B_n}{C_n} = \frac{Y_{n-1}(\lambda_2 a)J_n(\lambda_1 a) - \frac{\lambda_1}{\lambda_2}J_{n-1}(\lambda_1 a)Y_n(\lambda_2 a)}{\frac{\lambda_1}{\lambda_2}J_{n-1}(\lambda_1 a)J_n(\lambda_2 a) - J_{n-1}(\lambda_2 a)J_n(\lambda_1 a)}\,. \tag{5.28}$$

This equation shall be defined as $\beta(n, \lambda_1, \lambda_2, a)$

$$\boxed{\beta(n, \lambda_1, \lambda_2, a) \equiv \frac{Y_{n-1}(\lambda_2 a)J_n(\lambda_1 a) - \frac{\lambda_1}{\lambda_2}J_{n-1}(\lambda_1 a)Y_n(\lambda_2 a)}{\frac{\lambda_1}{\lambda_2}J_{n-1}(\lambda_1 a)J_n(\lambda_2 a) - J_{n-1}(\lambda_2 a)J_n(\lambda_1 a)}}\,. \tag{5.29}$$

Now the two unused boundary conditions are used. Equation (5.24) is divided by (5.20) to give

$$\frac{\lambda_2}{\lambda_3}\frac{B_n J_{n-1}(\lambda_2 b) + C_n Y_{n-1}(\lambda_2 b)}{B_n J_n(\lambda_2 b) + C_n Y_n(\lambda_2 b)} = \frac{D_n J_{n-1}(\lambda_3 b) + E_n Y_{n-1}(\lambda_3 b)}{D_n J_n(\lambda_3 b) + E_n Y_n(\lambda_3 b)}\,. \tag{5.30}$$

The numerator and denominator of the left-hand side of the equation are divided by C_n and the numerator and denominator of the right-hand side of the equation are divided by E_n to produce

$$\frac{\lambda_2}{\lambda_3}\frac{\frac{B_n}{C_n}J_{n-1}(\lambda_2 b) + Y_{n-1}(\lambda_2 b)}{\frac{B_n}{C_n}J_n(\lambda_2 b) + Y_n(\lambda_2 b)} = \frac{\frac{D_n}{E_n}J_{n-1}(\lambda_3 b) + Y_{n-1}(\lambda_3 b)}{\frac{D_n}{E_n}J_n(\lambda_3 b) + Y_n(\lambda_3 b)}\,. \tag{5.31}$$

Substituting in equations (5.25) and (5.28) to this equation and multiplying the right by $\frac{-J_n(\lambda_3 c)}{-J_n(\lambda_3 c)}$ then gives

$$\frac{\lambda_2}{\lambda_3}\frac{\beta(n, \lambda_1, \lambda_2, a)J_{n-1}(\lambda_2 b) + Y_{n-1}(\lambda_2 b)}{\beta(n, \lambda_1, \lambda_2, a)J_n(\lambda_2 b) + Y_n(\lambda_2 b)} = \frac{Y_n(\lambda_3 l)J_{n-1}(\lambda_3 b) - J_n(\lambda_3 l)Y_{n-1}(\lambda_3 b)}{Y_n(\lambda_3 l)J_n(\lambda_3 b) - J_n(\lambda_3 l)Y_n(\lambda_3 b)}\,. \tag{5.32}$$

There is now a change to one variable so that the equation can be solved. The new

quantities are defined as

$$
\begin{aligned}
y = \lambda_3 l = \frac{\omega l}{c_3} &= \omega l \sqrt{\frac{\rho_3}{T}}\,, \\
\tau^2 = \frac{\rho_1}{\rho_2} &= \frac{\lambda_1^2}{\lambda_2^2} = \frac{c_2^2}{c_1^2}\,, \\
\sigma^2 = \frac{\rho_2}{\rho_3} &= \frac{\lambda_2^2}{\lambda_3^2} = \frac{c_3^2}{c_2^2}\,, \\
q = \frac{a}{b}\,, & \\
k = \frac{b}{l}\,. &
\end{aligned}
$$

It is noted that σ^2 and τ^2 are a fixed ratio equal to the ratio of densities and k and q are equal to the ratio of the radii.

The new quantities are now subsituted into equation (5.32) and this gives an equation that can numerically solve for a given σ^2, τ^2, k and q. This is the equation whose solutions are the frequency eigenvalues:

$$
\boxed{\sigma \frac{\beta(n,y) J_{n-1}(\sigma k y) + Y_{n-1}(\sigma k y)}{\beta(n,y) J_n(\sigma k y) + Y_n(\sigma k y)} = \frac{Y_n(y) J_{n-1}(k y) - J_n(y) Y_{n-1}(k y)}{Y_n(y) J_n(k y) - J_n(y) Y_n(k y)}\,,} \tag{5.33}
$$

where

$$
\boxed{\beta(n,y) \equiv \frac{Y_{n-1}(\sigma k q y) J_n(\sigma \tau k q y) - \tau J_{n-1}(\sigma \tau k q y) Y_n(\sigma k q y)}{\tau J_{n-1}(\sigma \tau k q y) J_n(\sigma k q y) - J_{n-1}(\sigma k q y) J_n(\sigma \tau k q y)}\,.} \tag{5.34}
$$

Note that the eigenvalue equation needs both $k \neq 1$ and, from the β term, $\tau \neq 1$ to be defined.

The 2-density case can be solved in two ways from this 3-density model. If

$$
\begin{aligned}
k\,q &= k_{\text{2-density}} \\
\sigma &= 1 \\
\tau &= \sigma_{\text{2-density}}
\end{aligned}
$$

and equation (5.33) is solved then the eigenvalues will be the eigenvalues of the 2-density case. Alternatively, if

$$
\begin{aligned}
\sigma\,\tau &= \sigma_{\text{2-density}} \\
k &= k_{\text{2-density}} \\
q &= 1
\end{aligned}
$$

the 3-density model can still solve the 2-density case. If $\sigma\,\tau = 1$ then the 1-density case can also be solved with this method.

The results from the 3-density model for both the 2-density and 1-density cases are identical to their respective models.

Equation (5.33) will be solved for y, which can in turn be used to find either w, l, ρ_3 or T if the others are known. If this equation is defined there will be an infinite number solutions for a given σ, τ, k, q and each n. As in the previous cases the jth root of equation (5.33) will be y_{nj} where $j = 1$ is the first root greater than 0.

For each distinct y_{nj} there will be different ratios of A_{nj}, B_{nj}, C_{nj}, D_{nj} and E_{nj}. Just one coefficient, A_{nj}, is wanted which will be the amplitude of the system. B_{nj}, C_{nj}, D_{nj} and E_{nj} are now found in terms of A_{nj}.

To start with B_{nj} and C_{nj} will be obtained in terms of A_{nj}. The equation (5.28) will be rearranged to get $B_{nj} = \beta(y_{nj})C_n$ and substituted into equation (5.19) getting the equation

$$A_{nj}J_n(\sigma\tau kqy_{nj}) = \beta(y_{nj})C_nJ_n(\sigma kqy_{nj}) + C_nY_n(\sigma kqy_{nj})\,. \tag{5.35}$$

If this is rearranged then the equation provides C_{nj} in terms of A_{nj}:

$$C_{nj} = A_{nj}\frac{J_n(\sigma\tau kqy_{nj})}{\beta(y_{nj})J_n(\sigma kqy_{nj}) + Y_n(\sigma kqy_{nj})}\,. \tag{5.36}$$

Again a substitution is made from equation (5.28) $B_{nj} = \beta(n, y)C_n$ this time into equation (5.35). B_{nj} is solved in terms of A_{nj} to become

$$B_{nj} = A_{nj}\frac{\beta(y_{nj})J_n(\sigma\tau kqy_{nj})}{\beta(y_{nj})J_n(\sigma kqy_{nj}) + Y_n(\sigma kqy_{nj})}\,. \tag{5.37}$$

The next stage is to find D_{nj} in terms of A_{nj}. The above values of B_{nj} and C_{nj} are substituted, along with the rearranged equation (5.18) $E_{nj} = -D_{nj}\frac{J_n(y_{nj})}{Y_n(y_{nj})}$, into equation (5.20), getting

$$\begin{aligned} D_{nj}J_n(ky_{nj}) - D_{nj}\frac{J_n(y_{nj})}{Y_n(y_{nj})}Y_n(ky_{nj}) =& A_{nj}\frac{\beta(y_{nj})J_n(\sigma\tau kqy_{nj})}{\beta(y_{nj})J_n(\sigma kqy_{nj}) + Y_n(\sigma kqy_{nj})}J_n(\sigma ky_{nj}) \\ &+ A_{nj}\frac{J_n(\sigma\tau kqy_{nj})}{\beta(y_{nj})J_n(\sigma kqy_{nj}) + Y_n(\sigma kqy_{nj})}Y_{nj}(\sigma ky_{nj})\,. \end{aligned} \tag{5.38}$$

This is rearranged to produce the result of D_{nj} in terms of A_{nj}:

$$D_{nj} = A_{nj}\frac{\beta(y_{nj})J_n(\sigma ky_{nj}) + Y_n(\sigma ky_{nj})}{\beta(y_{nj})J_n(\sigma kqy_{nj}) + Y_n(\sigma kqy_{nj})}\frac{J_n(\sigma\tau kqy_{nj})Y_n(y_{nj})}{J_n(ky_{nj})Y_n(y_{nj}) - J_n(y_{nj})Y_n(ky_{nj})}\,. \tag{5.39}$$

Using the same method to find E_{nj} gives

$$E_{nj} = A_{nj}\frac{\beta(y_{nj})J_n(\sigma ky_{nj}) + Y_n(\sigma ky_{nj})}{\beta(y_{nj})J_n(\sigma kqy_{nj}) + Y_n(\sigma kqy_{nj})}\frac{J_n(\sigma\tau kqy_{nj})J_n(y_{nj})}{Y_n(ky_{nj})J_n(y_{nj}) - Y_n(y_{nj})J_n(ky_{nj})}\,. \tag{5.40}$$

The solutions of ψ now only depend on one amplitude, A_{nj}:

$$\psi_1(r,\theta) = A_{nj} J_n\left(\frac{\sigma\tau k q y_{nj}}{a}\, r\right)\sin(n\theta+\phi_n)\,, \tag{5.41}$$

$$\psi_2 = A_{nj}\frac{J_n(\sigma\tau k q y_{nj})}{\beta(y_{nj})J_n(\sigma k q y_{nj}) + Y_n(\sigma k q y_{nj})}\left[\beta(y_{nj})J_n\left(\frac{\sigma k y_{nj}}{b}r\right) + Y_n\left(\frac{\sigma k y_{nj}}{b}r\right)\right]\sin(n\theta+\phi_n)\,, \tag{5.42}$$

$$\begin{aligned}\psi_3 = A_{nj}&\frac{J_n(\sigma\tau k q y_{nj})\left[\beta(y_{nj})J_n(\sigma k y_{nj}) + Y_n(\sigma k y_{nj})\right]}{\beta(y_{nj})J_n(\sigma k q y_{nj}) + Y_n(\sigma k q y_{nj})}\\ &\times\left[\frac{Y_n(y_{nj})}{J_n(k y_{nj})Y_n(y_{nj}) - J_n(y_{nj})Y_n(k y_{nj})}J_n\left(\frac{y_{nj}}{l}r\right)\right.\\ &\left.+\frac{J_n(y_{nj})}{Y_n(k y_{nj})J_n(y_{nj}) - Y_n(y_{nj})J_n(k y_{nj})}Y_n\left(\frac{y_{nj}}{l}r\right)\right]\sin(n\theta+\phi_n)\,.\end{aligned} \tag{5.43}$$

5.2 Tuning the 3-Density Drum

The set of solutions to the eigenvalue equation (5.33) are denoted y_{nj}. Each solution is related to the frequency by the equation

$$y_{nj} = 2\pi f\, l\sqrt{\frac{\rho_3}{T}}\,. \tag{5.44}$$

l, ρ_3 and T are constants so there is a linear relationship between y_{nj} and the frequency. As in the 2-density case, for the drum to be perfectly in tune all the harmonics have to be integer multiples of the fundamental frequency, ie. $\frac{y_{nj}}{y_{01}} = 1, 2, 3....$

Varying σ, τ, k and q will produce different solutions of y_{nj} and as these are varied the proximity of the values $\frac{y_{nj}}{y_{01}}$ to the integers also changes. The objective is to get the harmonics as close to the integers as possible and, as before, this is achieved with the error equation, which is defined as

$$\text{Harmonic Error} = \sum_{h=2}^{5}\sum_{d=1}^{D}\left(\frac{y_{nj}/y_{01} - h}{h}\right)^2, \tag{5.45}$$

where h is the integer value of the harmonic that ψ_{nj} is closest to and D is the number of degenerate modes. As in the two-density model harmonics $h \geq 6$ are ignored.

Minimizing the Harmonic Error produces a significantly greater problem when four, as opposed to two, constants can be varied. A method of minimizing the error by varying one constant at a time is impossible due to the erratic nature of the function, caused by the large number of Bessel function terms on both the numerator and denominator. A brute force method is used here for minimizing the error. A set of values for each of the constants σ, τ, k and q are input into a Maple 12 program, written to trial every possible permutation of these sets and return an error value for each set (C.3). The program then selects the value with the lowest error and returns the error, along with the constants that produced it. After the program is run with the initial sets of parameters another set of parameters are input. These are chosen so the parameter that produced the minimum

error in the previous program run is the median value of the new run and so the intervals between the values in each set are reduced. Fine tuning is then done after this to get the minimum error when the parameters are adjusted to three significant figures.

It is recognised that this method is not guaranteed to locate the global minimum. To do this, a calculation would be needed with a number of permutations that would be orders of magnitude greater, requiring a considerably more powerful computer and a large amount of time available to access it.

After some sampling runs, using the two-density model and the physical tabla as guidelines, it was decided to do two initial runs. This decision was made based on the limited available time and computing power, along with the experimentally found values for the tabla. The first set of parameters were chosen to be

$$\begin{array}{cccc} \sigma & \tau & k & q \\ [2.6, 2.7 \ldots 4.1] & [1.01, 1.06 \ldots 1.36] & [0.3, 0.35 \ldots 0.7] & [0.3, 0.35 \ldots 0.7] \end{array}, \tag{5.46}$$

and the second set

$$\begin{array}{cccc} \sigma & \tau & k & q \\ [1.01, 1.06 \ldots 1.36] & [2.5, 2.6 \ldots 4.0] & [0.3, 0.35 \ldots 0.7] & [0.3, 0.35 \ldots 0.7] \end{array}. \tag{5.47}$$

After this, runs with smaller intervals, centered around the lowest value of each set, were made to locate a minimum.

When the ψ_{03} mode was placed at the 6^{th} harmonic the optimal parameters were found to be $\sigma = 2.81$, $\tau = 1.06$, $k = 0.390$ and $q = 0.339$. These parameters produce an error of 0.0015487. In this case the minimal error is not greatly reduced from the two-density model (error $= 0.001886$) and despite the extra calculations needed the more complex model produces only a marginally superior result.

When the ψ_{03} mode was placed at the 5^{th} harmonic the optimal parameters were found to be $\sigma = 4.62$, $\tau = 1.21$, $k = 0.456$ and $q = 0.6132$; these parameters produce an error of 0.00070534. With this configuration the minimal error is significantly reduced from the two-density model and the 6^{th} harmonic 3-density model, producing an error of 0.0044226.

Despite the simplest model of the tabla (the 2-density model) achieving considerably better harmonicity with the ψ_{03} mode placed at the 6^{th} harmonic, when the more realistic 3-density model is used the ψ_{03} mode placed at the 5^{th} harmonic produces a significantly lower error. This explains why the tabla possesses its particular harmonics.

As this method isn't guaranteed to find the global minimum, if different sets of parameters were chosen then the method may produce a lower error. The relative frequencies for the different modes of vibration are given in Table 5.1.

The real tabla is not perfectly harmonic as the harmonics depart slightly from the integer ratios. To model the tabla the harmonic values of the actual tabla must be reproduced. As the effect of the air pressure inside the tabla is not modelled the experimental values with the shell opened out is relevant to this model (Table 1.1). If the error is calculated by using the distance of the harmonics from the experimentally determined values then

	Frequency ratio		
Mode	2-density drum $\sigma = 2.84 \quad k = 0.385$	3-density drum ψ_{03} at 6^{th} $\sigma = 2.81 \quad \tau = 1.06$ $k = 0.390 \quad q = 0.339$	3-density drum ψ_{03} at 5^{th} $\sigma = 4.62 \quad \tau = 1.21$ $k = 0.456 \quad q = 0.613$
ψ_{01}	1.00	1.00	1.00
ψ_{11}	1.95	1.96	1.96
ψ_{21}	2.98	2.99	2.99
ψ_{02}	3.04	2.97	2.99
ψ_{12}	3.99	3.99	3.99
ψ_{31}	4.03	4.04	4.02
ψ_{22}	4.91	4.94	5.01
ψ_{41}	5.06	5.07	5.05
ψ_{13}	5.12	5.12	-
ψ_{03}	-	-	5.04
Error	0.0018906	0.0015487	0.00070534

Table 5.1: Comparison of error with respect to perfect harmonicity from a 2-density and a 3-density model

different values for the frequency ratios are produced when the error is minimized. The ψ_{03} 5^{th} harmonic is used to replicate the properties of the real-world tabla. As in the experimental results the 2^{nd} harmonic (y_{11}) is defined with a frequency ratio of 2.00. To give the same significance to the overall error, and acknowledging the fact that the fundamental frequency has a lower amplitude in practice than the 2^{nd} harmonic, the error for the ψ_{01} root is weighted

$$\text{Error}_{01} = \left(\frac{2y_{01}/y_{11} - 1.03}{2} \right)^2 . \tag{5.48}$$

The other roots have the same weighting as before.

The result of the error minimization when the error is taken with respect to the experimental values produces an error of 0.00024740 when the parameters are $\sigma = 2.74$, $\tau = 1.14$, $k = 0.476$ and $q = 0.513$. The frequency ratios for the modes of vibration are shown below in Table 5.2.

Table 5.2 shows that there is excellent agreement between the optimized 3-density model and the experimental values of the frequency ratios for the tabla. The 3-density model for the tabla produces results that model the right-handed tabla to a high degree of accuracy. The results are considerably better, with a significantly lower error, than the 2-density model and the 3-density model also better replicates the physical properties of the tabla. If the resulting frequencies for each model are listened to on the enclosed CD then it can be heard that, with the correct parameters, the 5^{th} harmonic 3-density model creates overtones that are more harmonic than a 2-density model.

	Frequency ratio	
Mode	Experimental values	3-density drum $\sigma = 2.74 \quad \tau = 1.14$ $k = 0.476 \quad q = 0.513$
ψ_{01}	1.03	1.06
ψ_{11}	2.00	2.00
ψ_{21}	3.00	2.99
ψ_{02}	3.00	3.00
ψ_{12}	4.00	4.00
ψ_{31}	4.00	4.03
ψ_{41}	5.03	5.04
ψ_{03}	5.04	5.05
ψ_{22}	5.08	5.08
Error	0	0.00024740

Table 5.2: Comparison of harmonic frequencies with the error calculated with respect to the harmonics from experimental results

5.2.1 Bringing the Parameter Values Within their Physical Limits

To get a wholly accurate model of the tabla, not only do the harmonics have to match the harmonics of the tabla but also the experimentally determined values for the radius and density ratios. The values of these are given by Ramakrishna and Sondhi as $0.45 < k < 0.55$ and $3 < \sigma_s < 4$. k has the same representation in both the 2 and 3-density models but due to the extra higher density region in the 3-density model the value of σ_s must be calculated from σ, τ and q. σ_s is assumed to be calculated from the average density of the syahi and is equal to σ for the 2-density model, but for the 3-density model it is defined as

$$\sigma_s^2 = \frac{\rho_s}{\rho_3}\,, \tag{5.49}$$

where ρ_s is the average density of the combined inner two regions relative to the outer membrane. The 2-dimensional density for the syahi ρ_s is given by

$$\rho_s = \frac{\text{Mass}}{\text{Area}} = \frac{\sum_{i=1}^{n} \rho_i \text{Area}_i}{\text{Area}}\,. \tag{5.50}$$

For the inner two regions of the 3-density model this becomes

$$\rho_s = \frac{\rho_1 \pi a^2 + \rho_2 \pi (b^2 - a^2)}{\pi b^2}\,. \tag{5.51}$$

Using $q = \frac{a}{b}$ this simplifies to

$$\rho_s = \rho_1 q^2 + \rho_2 - \rho_2 q^2\,. \tag{5.52}$$

Factorizing out ρ_2 and with the identity $\tau^2 = \frac{\rho_1}{\rho_2}$ this gives

$$\rho_s = \left(\frac{\rho_1}{\rho_2} q^2 + 1 - q^2\right) \rho_2\,, \tag{5.53}$$

and then

$$\rho_s = \left[q^2(\tau^2 - 1) + 1\right] \rho_2\,. \tag{5.54}$$

If this is substituted back into the equation (5.49) the result is

$$\sigma_s^2 = \left[q^2(\tau^2 - 1) + 1\right] \frac{\rho_2}{\rho_3} \,. \tag{5.55}$$

Using $\sigma^2 = \frac{\rho_2}{\rho_3}$ this becomes

$$\sigma_s^2 = \left[q^2(\tau^2 - 1) + 1\right] \sigma^2 \,. \tag{5.56}$$

This equation allows the calculation of σ_s from the parameters of the 3-density model. For the parameters that produce the minimal error with respect to the experimental values, σ_s evaluates to 2.85 : outside the real-world values. The optimal parameters within the allowed values of σ_s are therefore calculated (giving $\sigma_s = 3.01$ with $\sigma = 2.88$, $\tau = 1.15$, $k = 0.480$ and $q = 0.526$). Both values of k fall comfortably within the real world values.

	Frequency ratio		
Mode	Experimental values	3-density drum minimal error $\sigma = 2.74$ $\tau = 1.14$ $k = 0.476$ $q = 0.513$	3-density drum within σ_s values $\sigma = 2.88$ $\tau = 1.15$ $k = 0.480$ $q = 0.526$
ψ_{01}	1.03	1.06	1.06
ψ_{11}	2.00	2.00	2.00
ψ_{21}	3.00	2.99	2.99
ψ_{02}	3.00	3.00	3.01
ψ_{12}	4.00	4.00	4.00
ψ_{31}	4.00	4.03	4.03
ψ_{41}	5.03	5.04	5.04
ψ_{03}	5.04	5.05	5.08
ψ_{22}	5.08	5.08	5.08
Error	0	0.00024740	0.00029252

Table 5.3: Comparison of harmonic frequencies with the error calculated with respect to the harmonics from experimental results, including the values when the parameters are within their physical limits

Table 5.3 shows that if the parameters are within the real world limits then the agreement with the experimental values is only marginally decreased. If this restriction is placed on the parameters then the model still provides good agreement with the experimentally determined frequency ratios.

5.2.2 Summary

The 3-density model provides a very good method for replicating the eigenfrequency ratios of the right-handed tabla and can greatly reduce the harmonic error from the 2-density model. The model can almost exactly reproduce the experimental harmonic frequencies but the density ratio of the syahi and membrane falls outside the experimental values. It is noted, however, that the precision of the parameters that produced these results would be difficult to achieve using the construction techniques of tabla-makers (see Section 3.2.1). If the density ratio is limited to the experimental values the harmonic error is slightly, but

not greatly, increased. It is audibly difficult to discern a difference between these models and the experimental values (hear enclosed CD).

5.3 Graphs of the Vibrational Modes of the 3-Density Model

The vibrational modes for the 3-density model, optimized to produce minimal error with respect to the experimental values for the tabla ($\sigma = 2.74$, $\tau = 1.14$, $k = 0.476$, $q = 0.513$) are shown below.

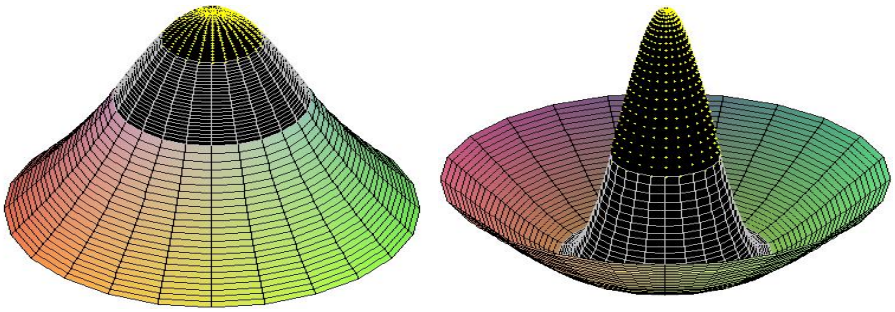

(a) ψ_{01} (b) ψ_{02}

Figure 5.2: $\psi_{01}(r, \theta)$ and $\psi_{02}(r, \theta)$ for 3-density concentric drum

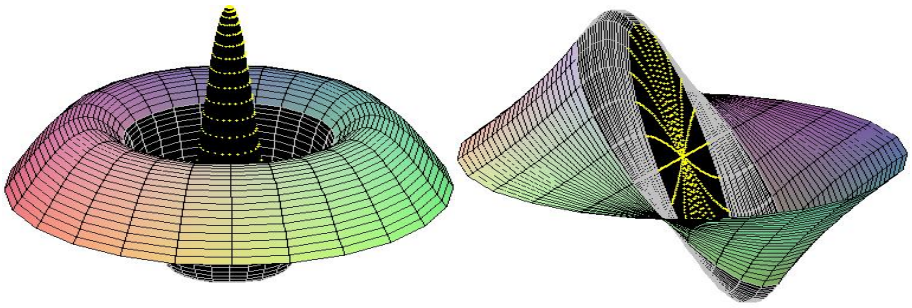

(a) ψ_{03} (b) ψ_{11}

Figure 5.3: $\psi_{03}(r, \theta)$ and $\psi_{11}(r, \theta)$ for 3-density concentric drum

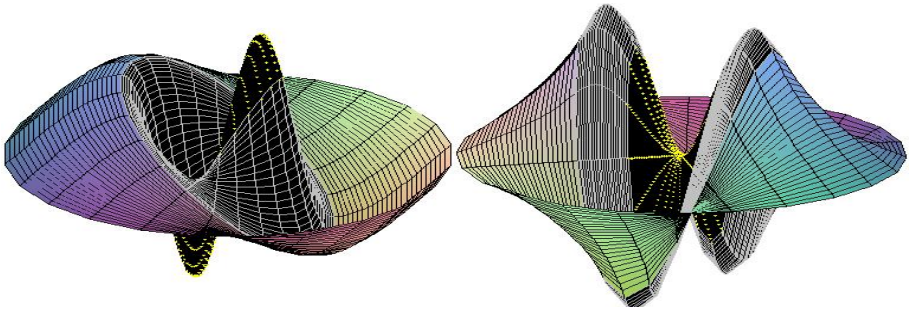

(a) ψ_{12} (b) ψ_{21}

Figure 5.4: $\psi_{12}(r,\theta)$ and $\psi_{21}(r,\theta)$ for 3-density concentric drum

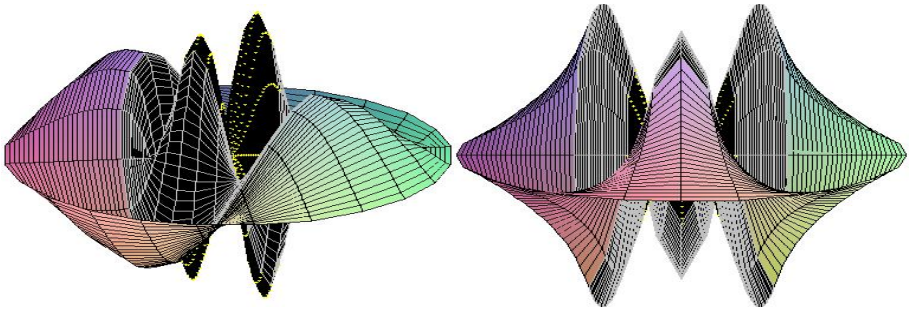

(a) ψ_{22} (b) ψ_{31}

Figure 5.5: $\psi_{22}(r,\theta)$ and $\psi_{31}(r,\theta)$ for 3-density concentric drum

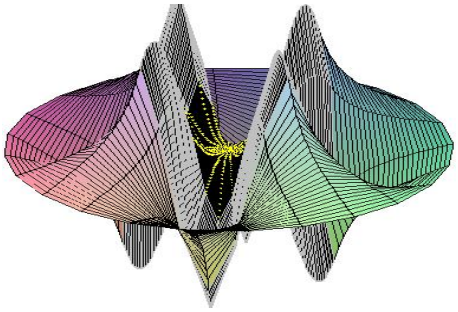

(a) ψ_{41}

Figure 5.6: $\psi_{41}(r,\theta)$ for 3-density concentric drum

Chapter 6

A Damping Term

In a real world system damping affects the movement of the simple harmonic oscillator. This effect can be included in the model for a drum.

When a force opposes the movement of the oscillating sytem, damped harmonic motion occurs. In a real world system there can be many contributing factors resisting the motion. The frictional force produced is linearly proportional to the velocity [FR]:

$$F = -\mu \dot{z} \tag{6.1}$$

where μ is the damping coefficient and $\dot{z}$ is the velocity. The minus sign is present as the force is resisting the motion. If this equation is made equal to Newton's second law and the acceleration is made the subject then the equation becomes $\ddot{z} = -\frac{\mu}{m}\dot{z}$. If this is included into the 2D wave equation, as used for modelling the tabla, the wave equation with the damping term is

$$\ddot{z} = c^2 \nabla^2 z - \frac{\mu}{m}\dot{z}\,, \tag{6.2}$$

If separation of variables is used as before (setting each side equal to the constant $-\omega^2$), and the damping term is moved to the left, the result is

$$\frac{h_{tt}(t)}{h(t)} + \frac{\mu}{m}\frac{h_t(t)}{h(t)} = c^2 \frac{\nabla^2 \psi(r,\theta)}{\psi(r,\theta)} = -\omega^2\,. \tag{6.3}$$

This equation is rearranged to find the solution of h:

$$h_{tt} + \frac{\mu}{m} h_t + \omega^2 h = 0\,. \tag{6.4}$$

This can be written

$$\ddot{h} + 2\alpha \dot{h} + \omega^2 h = 0\,, \tag{6.5}$$

where $\alpha = \frac{\mu}{2m}$. To solve this equation a solution in the form $h = Ae^{\gamma t + \varphi_1}$ can be taken. This gives, when differentiated and substituted into equation (6.5),

$$Ae^{\gamma t+\varphi_1}(\gamma^2 + 2\alpha\gamma + \omega^2) = 0\,. \tag{6.6}$$

This is solved as a quadratic equation and gives the solutions

$$\gamma = -\alpha \pm \sqrt{\alpha^2 - \omega^2}\,, \tag{6.7}$$

which can be rewritten as

$$\gamma = -\alpha \pm i\sqrt{\omega^2 - \alpha^2}\,. \tag{6.8}$$

The two roots being referred to as γ_1 and γ_2, this is then put back into $h = Ae^{\gamma t+\varphi_1}$ to give the time dependent displacement as the general solution

$$h = Be^{\gamma_1 t+\varphi_1} + Ce^{\gamma_2 t+\varphi_1}\,. \tag{6.9}$$

Substituting in the two roots and factorizing produces

$$h = e^{-\alpha t}\Big(Be^{i(\sqrt{\omega^2-\alpha^2}\,t+\varphi_2)} + Ce^{-i(\sqrt{\omega^2-\alpha^2}\,t-\varphi_2)}\Big)\,. \tag{6.10}$$

As shown previously in Chapter 2 (2.9) this equation can be written in the form

$$h = Ae^{-\alpha t}\cos(\sqrt{\omega^2 - \alpha^2}\,t + \varphi)\,. \tag{6.11}$$

The angular frequency of this system is therefore

$$\omega_d = \sqrt{\omega^2 - \alpha^2}\,, \tag{6.12}$$

with ω being the angular frequency of an undamped system. From equation (6.11) it can be seen that the amplitude of the system decays in the form $Ae^{-\alpha t}$.

It is noted that for harmonic motion to occur the system must be underdamped. An overdamped or critically damped system will not oscillate. Therefore $\omega^2 - \alpha^2 > 0$. If equation (6.12) is written instead in terms of frequency using $\omega = 2\pi f$ then the result is

$$f_d = \sqrt{f^2 - \frac{\alpha^2}{4\pi^2}}\,. \tag{6.13}$$

If this is written as the natural frequency multiplied by a damping term it becomes

$$f_d = f\sqrt{1 - \frac{\alpha^2}{4\pi^2 f^2}}\,. \tag{6.14}$$

An approximate value of α was found by varying the damping term in a synthesizing program and aurally determining when the decay time seemed closest to the sound of a tabla. The result found as that $\alpha \approx 6.5$. This value is used in equation (6.14), along with the natural frequency of 174.6 Hz. The damped frequency is then calculated to be 174.597 Hz, which is indistinguishable to the human ear from the natural frequency. It can be seen from equation (6.14) that the effect on the higher harmonics will be even smaller. The damping of the membrane will therefore have a negligible effect on the frequency and no correction needs to be made to the models.

Chapter 7

The Variational Method for the 2-Density Model

Here a different method is used to solve the 2-density model of the tabla. This method also has the potential to find the frequency eigenvalues of the asymmetric left-handed tabla. The method used for the two and three density models cannot be used for the asymmetric case as there is no solution to the partial differential equation that results from the boundary conditions.

The left-handed tabla is of a similar composition to the right-handed tabla, but is loaded in an eccentric manner. Bipolar coordinates can be used to describe the eccentric loading of the membrane. The method used here includes the bipolar coordinate system which allows the asymmetric case to also be solved using the same method. This method of finding the vibrational modes of the Indian drum was first set out by Sarojini and Rahman [SR].

Using the modified bipolar coordinates and the scale factor which are derived in Appendix B, along with the results of bipolar coordinates, the following operators result:

$$\nabla^2 = \frac{\left(\frac{r^2}{4\alpha} + \alpha - r\cos\theta\right)^2}{\alpha^2}\left(\frac{\partial^2}{\partial r^2} + \frac{1}{r}\frac{\partial}{\partial r} + \frac{1}{r^2}\frac{\partial^2}{\partial\theta^2}\right), \tag{7.1}$$

$$\nabla = \frac{\frac{r^2}{4\alpha} + \alpha - r\cos\theta}{\alpha}\left(\frac{\partial}{\partial r}\hat{\mathbf{r}} + \frac{1}{r}\frac{\partial}{\partial\theta}\hat{\theta}\right), \tag{7.2}$$

$$dS = \frac{\alpha^2}{\left(\frac{r^2}{4\alpha} + \alpha - r\cos\theta\right)^2} r dr d\theta\,. \tag{7.3}$$

By employing these modified bipolar coordinates, the same wave equation and boundary conditions can describe the asymmetric tabla.

These are

$$\nabla^2\psi_1 + \lambda_1^2\psi_1 = 0 \quad \text{for} \quad 0 \le r \le a\,, \tag{7.4}$$

$$\nabla^2\psi_2 + \lambda_2^2\psi_2 = 0 \quad \text{for} \quad a \le r \le b\,, \tag{7.5}$$

where

$$\lambda_1 = \frac{\omega}{c_1} = \omega\sqrt{\frac{\rho_1}{T}} \qquad \text{when} \quad 0 \le r \le a\,,$$
$$\lambda_2 = \frac{\omega}{c_2} = \omega\sqrt{\frac{\rho_2}{T}} \qquad \text{when} \quad a \le r \le b\,,$$

and the boundary conditions are

$$\psi(r,\theta) \in \mathbb{R} \quad \text{when} \quad 0 \le r \le b\,, \tag{7.6}$$
$$\psi_2(b,\theta) = 0\,, \tag{7.7}$$
$$\psi_1(a,\theta) = \psi_2(a,\theta)\,, \tag{7.8}$$
$$\frac{\partial}{\partial r}\psi_1(a,\theta) = \frac{\partial}{\partial r}\psi_2(a,\theta)\,, \tag{7.9}$$
$$\psi(r,\theta) = \psi(r,\theta+2\pi n)\,. \tag{7.10}$$

However, with the modified bipolar scale factor present in the Laplacian, the wave equation is not separable unless the scale factor is 1, which only happens in the concentric case when $\alpha \to \infty$. This means a different method must be used to solve the equation if the possibility of solving the asymmetric case is to remain open. The method used is the Variational Method.

7.1 The Variational Method for solving the Left-Handed Indian Drum

The wave equation for the drum is written in the form of a single equation

$$\nabla^2\psi + \frac{\omega^2\rho}{T}\psi = 0\,, \tag{7.11}$$

where

$$\rho = \begin{cases} \rho_1, & \text{if} \quad 0 \le r < a\,, \\ \rho_2, & \text{if} \quad a \le r \le b\,. \end{cases} \tag{7.12}$$

If equation (7.11) is rearranged then it produces

$$-\frac{\omega^2}{T} = \frac{\nabla^2\psi}{\rho\psi}\,. \tag{7.13}$$

The right-hand side can then be multiplied by $\frac{\psi}{\psi}$, then both the numerator and denominator integrated with respect to the surface, taken over the whole drum membrane:

$$-\frac{\omega^2}{T} = \frac{\int \psi\nabla^2\psi\, dS}{\int \rho\,\psi^2\, dS}\,. \tag{7.14}$$

It can be shown, using the Divergence Theorem, that the numerator is equal to

$$-\int \psi\nabla^2\psi\, dS = \int (\nabla\psi)^2\, dS\,. \tag{7.15}$$

This is demonstrated below.

The Divergence Theorem states that

$$\int_{\Omega} (\nabla \cdot \mathbf{F})\, dV = \int_{\partial\Omega} \mathbf{F} \cdot \mathbf{n}\, dS\,. \tag{7.16}$$

If $\mathbf{F} = \psi\nabla\psi$ then the divergence theorem gives

$$\int_{\Omega} (\nabla \cdot (\psi\nabla\psi))\, dV = \int_{\partial\Omega} \psi\nabla\psi \cdot \mathbf{n}\, dS\,. \tag{7.17}$$

Using the identity $\nabla \cdot (\phi\mathbf{A}) = \nabla\phi \cdot \mathbf{A} + \phi\nabla \cdot \mathbf{A}$ the obtained result is

$$\int_{\Omega} \nabla\psi \cdot \nabla\psi dV + \int_{\Omega} \psi\nabla^2\psi dV = \int_{\partial\Omega} \psi\nabla\psi \cdot \mathbf{n}\, dS\,. \tag{7.18}$$

As boundary condition (7.6) states that $\psi = 0$ on the boundary, this means that $\int_{\partial\Omega} \nabla\psi \cdot \mathbf{n}\, dS = 0$, leaving

$$\int_{\Omega} \nabla\psi \cdot \nabla\psi\, dV + \int_{\Omega} \psi\nabla^2\psi\, dV = 0\,. \tag{7.19}$$

This can be rewritten as

$$-\int_{\Omega} \psi\nabla^2\psi\, dV = \int_{\Omega} (\nabla\psi)^2\, dV\,. \tag{7.20}$$

ψ and the scale factor are functions of only two variables (r and θ) and $dV = dS\, dz$. This means the additional integration element dz will evaluate to the same constant on both sides of the equation. The constant then cancels out, leaving

$$-\int \psi\nabla^2\psi\, dS = \int (\nabla\psi)^2\, dS\,. \tag{7.21}$$

This shows that equation (7.15) holds. The right-hand side of this can, using equations (7.2) and (7.3), be written as

$$\int (\nabla\psi)^2\, dS = \int \left(\frac{\frac{r^2}{4\alpha} + \alpha - r\cos\theta}{\alpha} \left(\frac{\partial\psi}{\partial r}\hat{\mathbf{r}} + \frac{1}{r}\frac{\partial\psi}{\partial\theta}\hat{\theta} \right) \right)^2 \frac{\alpha^2}{\left(\frac{r^2}{4\alpha} + \alpha - r\cos\theta \right)^2} r dr d\theta\,. \tag{7.22}$$

The scale factors and orthogonal vectors cancel out when the bracket is squared and leaves

$$\int (\nabla\psi)^2\, dS = \int \left[\left(\frac{\partial\psi}{\partial r} \right)^2 + \frac{1}{r^2} \left(\frac{\partial\psi}{\partial\theta} \right)^2 \right] r dr d\theta\,. \tag{7.23}$$

The scale factor has been removed and the equation is therefore identical to the orthodox polar coordinate equation. Equation (7.14) now becomes

$$\boxed{\frac{\omega^2}{T} = \frac{\int \left[\left(\frac{\partial\psi}{\partial r} \right)^2 + \frac{1}{r^2} \left(\frac{\partial\psi}{\partial\theta} \right)^2 \right] r dr d\theta}{\int \rho\, \psi^2\, dS}\,.} \tag{7.24}$$

As in the first method for solving the 2-density drum, dimensionless quantities are now introduced:

$$r = bs\,, \tag{7.25}$$

$$x = \lambda_2 b = \frac{\omega b}{c_2}\,, \tag{7.26}$$

$$\sigma^2 = \frac{\rho_1}{\rho_2} = \frac{\lambda_1^2}{\lambda_2^2}\,, \tag{7.27}$$

$$k = \frac{a}{b}\,, \tag{7.28}$$

$$\Delta = \frac{b}{2\alpha}\,. \tag{7.29}$$

The scale factor is divided through on both the numerator and denominator by α to produce

$$\frac{1}{1-\frac{2r\cos\theta}{2\alpha}+\frac{r^2}{4\alpha^2}} = \frac{1}{1-2\Delta s\cos\theta+\Delta^2 s^2}\,.$$

and the dimensionless quantities are subsituted into equation (7.24). Together, this gives

$$\frac{x^2}{b^2\rho_2} = \frac{\int_0^{2\pi}\int_0^{k}\left[\frac{1}{b^2}\left(\frac{\partial\psi_1}{\partial s}\right)^2+\frac{1}{b^2s^2}\left(\frac{\partial\psi_1}{\partial\theta}\right)^2\right]b^2s\,dsd\theta+\int_0^{2\pi}\int_k^{1}\left[\frac{1}{b^2}\left(\frac{\partial\psi_2}{\partial s}\right)^2+\frac{1}{b^2s^2}\left(\frac{\partial\psi_2}{\partial\theta}\right)^2\right]b^2s\,dsd\theta}{\rho_1\int_0^{2\pi}\int_0^{k}\frac{\psi_1^2}{(1-2\Delta s\cos\theta+\Delta^2s^2)^2}b^2s\,dsd\theta+\rho_2\int_0^{2\pi}\int_k^{1}\frac{\psi_2^2}{(1-2\Delta s\cos\theta+\Delta^2s^2)^2}b^2s\,dsd\theta}\,. \tag{7.30}$$

The b s on the numerator cancel and the left-side b^2 cancels with the denominator b s. The ρ_2 is brought over the right-hand side, producing the equation

$$\boxed{x^2 = \frac{\int_0^{2\pi}\int_0^{k}\left[\left(\frac{\partial\psi_1}{\partial s}\right)^2+\frac{1}{s^2}\left(\frac{\partial\psi_1}{\partial\theta}\right)^2\right]s\,dsd\theta+\int_0^{2\pi}\int_k^{1}\left[\left(\frac{\partial\psi_2}{\partial s}\right)^2+\frac{1}{s^2}\left(\frac{\partial\psi_2}{\partial\theta}\right)^2\right]s\,dsd\theta}{\sigma^2\int_0^{2\pi}\int_0^{k}\frac{\psi_1^2}{(1-2\Delta s\cos\theta+\Delta^2s^2)^2}s\,dsd\theta+\int_0^{2\pi}\int_k^{1}\frac{\psi_2^2}{(1-2\Delta s\cos\theta+\Delta^2s^2)^2}s\,dsd\theta}\,.} \tag{7.31}$$

The scale factor disappears as Δ tends to zero and the equation becomes the variational integral for the concentric drum. A binomial expansion is now made on the square of the scale factor and terms of order Δ^3 or higher are discarded:

$$\frac{1}{(1-2\Delta s\cos\theta+\Delta^2s^2)^2} = 1+4\Delta s\cos\theta-2\Delta^2s^2+3(4\Delta^2s^2\cos^2\theta+O(\Delta^3)),$$

Using the identity $\cos 2\theta = 2\cos^2\theta - 1$ gives

$$\frac{1}{(1-2\Delta s\cos\theta+\Delta^2s^2)^2} = 1+4\Delta s\cos\theta-2\Delta^2s^2+3(2\Delta^2s^2(\cos 2\theta+1)+O(\Delta^3))\,.$$

This means the scale factor squared is now

$$\boxed{\frac{1}{(1-2\Delta s\cos\theta+\Delta^2s^2)^2} \approx 1+4\Delta s\cos\theta+4\Delta^2s^2+6\Delta^2s^2\cos 2\theta\,.} \tag{7.32}$$

As ψ is 2π periodic, it can be written in the form of a Fourier series:

$$\boxed{\begin{aligned}\psi_1(s,\theta) &= \sum_{n=0}^{\infty}\xi_n(s)\cos(n\theta)+\sum_{n=1}^{\infty}\eta_n(s)\sin(n\theta), \qquad 0\le s\le k\,, \qquad (7.33)\\ \psi_2(s,\theta) &= \sum_{n=0}^{\infty}\phi_n(s)\cos(n\theta)+\sum_{n=1}^{\infty}\chi_n(s)\sin(n\theta), \qquad k\le s\le 1\,. \qquad (7.34)\end{aligned}}$$

The functions ϕ_n and χ_n can have a singularity at $s=0$, as is the case with Bessel functions of the second kind.

The next stage is to substitute the Fourier series identities of ψ_1 and ψ_2 into equation (7.31) and evaluate the θ integrals. To start with, the θ integral from the term $\int_0^{2\pi}\int_0^{k}\left(\frac{\partial\psi_1}{\partial s}\right)^2 s\,ds d\theta$ is evaluated. $\left(\frac{\partial\psi_1}{\partial s}\right)^2$ is equal to

$$\begin{aligned}\left(\frac{\partial\psi_1}{\partial s}\right)^2 = &\left(\sum_{n=0}^{\infty}\sum_{m=0}^{\infty}\xi_n'(s)\xi_m'(s)\cos(n\theta)\cos(m\theta)\right)+\left(\sum_{n=1}^{\infty}\sum_{m=1}^{\infty}\eta_n'(s)\eta_m'(s)\sin(n\theta)\sin(m\theta)\right)\\ &+2\left(\sum_{n=1}^{\infty}\sum_{m=1}^{\infty}\xi_n'(s)\eta_m'(s)\cos(n\theta)\sin(m\theta)\right)+\xi_0'(s)\sum_{n=1}^{\infty}\eta_n'(s)\sin(n\theta) \qquad (7.35)\end{aligned}$$

This function is integrated with respect to θ in equation (7.31). One term of the above function shall be integrated at a time. The $\sum_{n=0}^{\infty}\sum_{m=0}^{\infty}\xi_n'(s)\xi_m'(s)\cos(n\theta)\cos(m\theta)$ term will be the first integrated and, to help notation, the definition

$$f^{\xi\xi}(s)=\sum_{n=0}^{\infty}\sum_{m=0}^{\infty}\xi_n'(s)\xi_m'(s)$$

is made. If the θ integral from equation (7.31) is evaluated for this term then, as $n,m\ge 0$, the result is

$$\int_0^{2\pi} f^{\xi\xi}(s)\cos(n\theta)\cos(m\theta)\,d\theta=\begin{cases}0\,, & \text{if} \quad n\ne m\,,\\ 2\pi f^{\xi\xi}(s)\,, & \text{if} \quad n=m=0\,,\\ \pi f^{\xi\xi}(s)\,, & \text{if} \quad n=m\ge 1\,.\end{cases} \qquad (7.36)$$

This allows the evaluated term to be written as

$$\int_0^{2\pi}\sum_{n=0}^{\infty}\sum_{m=0}^{\infty}\xi_n'(s)\xi_m'(s)\cos(n\theta)\cos(m\theta)\,d\theta=2\pi(\xi_0')^2+\pi\sum_{n=1}^{\infty}(\xi_n')^2 \qquad (7.37)$$

The term $\sum_{n=1}^{\infty}\sum_{m=1}^{\infty}\eta_n'(s)\eta_m'(s)\sin(n\theta)\sin(m\theta)$, from equation (7.35), gives a slightly different result when integrated with respect to θ between 0 and 2π as $n=m=0$

is not within the summation limits for this term. This time the definition $f^{\eta\eta}(s) = \sum_{n=1}^{\infty}\sum_{m=1}^{\infty}\eta_n'(s)\eta_m'(s)$ is made and the results are:

$$\int_0^{2\pi} f^{\eta\eta}(s)\sin(n\theta)\sin(m\theta)\,d\theta = \begin{cases} 0\,, & \text{if} \quad n \neq m\,, \\ \pi f^{\eta\eta}(s)\,, & \text{if} \quad n = m \geq 1\,. \end{cases} \tag{7.38}$$

This allows the term to be written as

$$\int_0^{2\pi}\sum_{n=1}^{\infty}\sum_{m=1}^{\infty}\eta_n'(s)\eta_m'(s)\sin(n\theta)\sin(m\theta)\,d\theta = \pi\sum_{n=1}^{\infty}(\eta_n')^2 \tag{7.39}$$

For the remaining two terms the integral evaluates to zero:

$$\int_0^{2\pi} 2\left(\sum_{n=1}^{\infty}\sum_{m=1}^{\infty}\xi_n'(s)\eta_m'(s)\cos(n\theta)\sin(m\theta)\right)d\theta = 0 \tag{7.40}$$

$$\int_0^{2\pi}\xi_0'(s)\sum_{n=1}^{\infty}\eta_n'(s)\sin(n\theta)\,d\theta = 0 \tag{7.41}$$

The evaluated θ integral for the function found in equation (7.35) is therefore just equations (7.37) and (7.39) added together, giving

$$\int_0^{2\pi}\left(\frac{\partial\psi_1}{\partial s}\right)^2 d\theta = 2\pi(\xi_0')^2 + \pi\sum_{n=1}^{\infty}(\xi_n')^2 + \pi\sum_{n=1}^{\infty}(\eta_n')^2 \tag{7.42}$$

The same method is used for the $\frac{1}{s^2}\left(\frac{\partial\psi_1}{\partial\theta}\right)^2$ term from equation (7.31) and a similar result is found. The differentiation with respect to θ causes the function to be multiplied by n^2, so there is no term for $n = 0$. The term evaluates to

$$\int_0^{2\pi}\frac{1}{s^2}\left(\frac{\partial\psi_1}{\partial\theta}\right)^2 d\theta = \pi\sum_{n=1}^{\infty}\frac{1}{s^2}\eta_n^2 n^2 + \pi\sum_{n=1}^{\infty}\frac{1}{s^2}\xi_n^2 n^2 \tag{7.43}$$

Adding (7.42) and (7.43) together gives the total ψ_1 part of the numerator, which is

$$2\pi\int_0^k s\,ds(\xi_0')^2 + \pi\int_0^k s\,ds\sum_{n=1}^{\infty}\left[(\xi_n')^2 + (\eta_n')^2 + \frac{1}{s^2}\left(\xi_n^2 n^2 + \eta_n^2 n^2\right)\right]. \tag{7.44}$$

Exactly the same result comes from ψ_2 and its respective functions, but with different integration limits. The resulting **total numerator** is

$$\boxed{\begin{aligned} &2\pi \int_0^k s\,ds(\xi_0')^2 + \pi \int_0^k s\,ds \sum_{n=1}^{\infty} \left[(\xi_n')^2 + (\eta_n')^2 + \frac{1}{s^2}\left(\xi_n^2 n^2 + \eta_n^2 n^2\right)\right] \\ &+ 2\pi \int_k^1 s\,ds(\phi_0')^2 + \pi \int_k^1 s\,ds \sum_{n=1}^{\infty} \left[(\phi_n')^2 + (\chi_n')^2 + \frac{1}{s^2}\left(\phi_n^2 n^2 + \chi_n^2 n^2\right)\right]. \end{aligned}} \tag{7.45}$$

The denominator of (7.31) produces a more complex result. Taking only ψ_1 to begin with, then ψ_1^2 in the denominator becomes

$$\begin{aligned} \psi_1^2 = &\sum_{n=0}^{\infty}\sum_{m=0}^{\infty} \xi_n(s)\xi_m(s)\cos(n\theta)\cos(m\theta) + \sum_{n=1}^{\infty}\sum_{m=1}^{\infty} \eta_n(s)\eta_m(s)\sin(n\theta)\sin(m\theta) \\ &+ 2\sum_{n=1}^{\infty}\sum_{m=1}^{\infty} \xi_n(s)\eta_m(s)\cos(n\theta)\sin(m\theta) + \xi_0(s)\sum_{n=1}^{\infty}\eta_n(s)\sin(n\theta) \end{aligned} \tag{7.46}$$

The ψ_1 term of the denominator (equation 7.31) with the scale factor included then becomes

$$\begin{aligned} \int_0^{2\pi} \psi_1^2(1 + 4\Delta^2 s^2 + 4\Delta s\cos\theta + 6\Delta^2 s^2\cos 2\theta)\,d\theta = &\int_0^{2\pi} \Big[\sum_{n=0}^{\infty}\sum_{m=0}^{\infty} \xi_n(s)\xi_m(s)\cos(n\theta)\cos(m\theta) \\ &+ \sum_{n=1}^{\infty}\sum_{m=1}^{\infty} \eta_n(s)\eta_m(s)\sin(n\theta)\sin(m\theta) + 2\sum_{n=1}^{\infty}\sum_{m=1}^{\infty} \xi_n(s)\eta_m(s)\cos(n\theta)\sin(m\theta) \\ &+ \xi_0(s)\sum_{n=1}^{\infty}\eta_n(s)\sin(n\theta)\Big](1 + 4\Delta^2 s^2 + 4\Delta s\cos\theta + 6\Delta^2 s^2\cos 2\theta)\,d\theta\,. \end{aligned} \tag{7.47}$$

The scale factor gives three different terms to multiply with ψ_1^2 and integrate: a constant, a $\cos\theta$ term and a $\cos 2\theta$ term. Different integrals are needed for when the scale factor has $\cos\theta$ and $\cos 2\theta$. For the $(1 + 4\Delta^2 s^2)$ term of the scale factor the same integrals as the numerator apply, giving the result

$$\sigma^2 \int_0^k (1 + 4\Delta^2 s^2)[2\pi\xi_0^2 + \pi\sum_{n=1}^{\infty}(\xi_n^2 + \eta_n^2)]s\,ds\,. \tag{7.48}$$

Finding the results of only the functions of θ, the $4\Delta s\cos\theta$ from the scale factor multiplies

with the ψ_1^2 to give integrals of

$$\int_0^{2\pi} \cos n\theta \cos m\theta \cos\theta d\theta = \frac{1}{4}\left(\frac{\sin((m-n-1)x)}{m-n-1} + \frac{\sin((m-n+1)x)}{m-n+1} + \frac{\sin((m+n-1)x)}{m+n-1} + \frac{\sin((m+n+1)x)}{m+n+1}\right)\Bigg|_0^{2\pi}, \quad (7.49)$$

$$\int_0^{2\pi} \sin n\theta \sin m\theta \cos\theta\, d\theta = \frac{1}{4}\left(\frac{\sin((m-n-1)x)}{m-n-1} + \frac{\sin((m-n+1)x)}{m-n+1} + \frac{\sin((m+n-1)x)}{m+n-1} + \frac{\sin((m+n+1)x)}{m+n+1}\right)\Bigg|_0^{2\pi}, \quad (7.50)$$

$$\int_0^{2\pi} \cos n\theta \sin m\theta \cos\theta\, d\theta = -\frac{1}{4}\left(\frac{\cos((m-n-1)x)}{m-n-1} + \frac{\cos((m-n+1)x)}{m-n+1} + \frac{\cos((m+n-1)x)}{m+n-1} + \frac{\cos((m+n+1)x)}{m+n+1}\right)\Bigg|_0^{2\pi}. \quad (7.51)$$

For the special case of $n = 0$ in the first term of equation (7.49), the integral is

$$\int_0^{2\pi} \cos m\theta \cos\theta d\theta = \frac{\sin\theta \sin m\theta + m\cos\theta\cos m\theta}{1-m^2}\Bigg|_0^{2\pi}. \quad (7.52)$$

Looking at the denominator in (7.52), the integral evaluates to zero unless $m = 1$. If the integral is calculated with $m = 1$ then a normal $\cos^2\theta$ integral results, which evaluates to π:

$$\int_0^{2\pi} \cos\theta\cos\theta d\theta = \int_0^{2\pi} \cos^2\theta d\theta = \pi\,. \quad (7.53)$$

The same value also exists for $m = 0$, so multiplying this by 2 for the $n, m = 0$ case of the $4\Delta s\cos\theta$ scale factor on the denominator produces

$$4\Delta s[2\pi\xi_0\xi_1]\,. \quad (7.54)$$

Now the sums of (7.49) to (7.51) have the limits $\sum_{m,n=1}^{\infty}$ as the $m, n = 0$ case has been solved. Equations (7.49) to (7.51) will all evaluate to 0 unless one of the denominators is zero. The conditions that must be satisfied are

$$m-n-1=0\,, \qquad m-n+1=0\,, \qquad m+n-1=0\,, \qquad m+n+1=0\,. \quad (7.55)$$

The third condition and fourth conditions can't be satisfied if $m, n \geq 1$, so the only conditions needed to find the integral are $m = n+1$ or $m = n-1$. Using this relation in equation (7.49) gives

$$\int_0^{2\pi} \cos n\theta \cos((n+1)\theta)\cos\theta\, d\theta = \frac{1}{8}\left(\frac{\sin 2nx}{n} + \frac{\sin(2(n+1)x)}{n+1} + 2x + \sin 2x\right)\Bigg|_0^{2\pi} = \frac{\pi}{2}\,. \quad (7.56)$$

This is multiplied by 2 as the other condition will have the same result, which gives

$$4\Delta s(\pi \sum_{n=1}^{\infty} \xi_n \xi_{n+1}) \,. \tag{7.57}$$

As the integral for $\sin n\theta \sin m\theta \cos\theta$ gives the same result, the function that result from the $\sin n\theta \sin m\theta \cos\theta$ is

$$4\Delta s(\pi \sum_{n=1}^{\infty} \eta_n \eta_{n+1}) \,. \tag{7.58}$$

The equation (7.51) evaluates to 0 when $n = m + 1$, $n = m - 1$ for $n, m \geq 1$. Similarly $\xi_0(s) \sum_{n=1}^{\infty} \eta_n(s) \sin(n\theta) \cos\theta$ evaluates to zero when integrated between 0 and 2π. These integrals will not contribute to the denominator.

The total denominator section for the $4\Delta s \cos\theta$ part of the scale factor is therefore

$$4\Delta s \left[2\pi \xi_0 \xi_1 + \pi \sum_{n=1}^{\infty} (\xi_n \xi_{n+1} + \eta_n \eta_{n+1}) \right] . \tag{7.59}$$

The term for the $6\Delta^2 s^2 \cos 2\theta$ part of the scale factor is derived in the same way and produces the term

$$6\Delta^2 s^2 \left[\frac{\pi}{2} (\xi_1^2 - \eta_1^2) + 2\pi \xi_0 \xi_2 + \pi \sum_{n=1}^{\infty} (\xi_n \xi_{n+2} + \eta_n \eta_{n+2}) \right] . \tag{7.60}$$

The total denominator part from ψ_1 is now

$$\sigma^2 \int_0^k s\, ds (1 + 4\Delta^2 s^2)[2\pi \xi_0^2 + \pi \sum_{n=1}^{\infty} (\xi_n^2 + \eta_n^2)] + 4\Delta s \left[2\pi \xi_0 \xi_1 + \pi \sum_{n=1}^{\infty} (\xi_n \xi_{n+1} + \eta_n \eta_{n+1}) \right]$$
$$+ 6\Delta^2 s^2 \left[\frac{\pi}{2} (\xi_1^2 - \eta_1^2) + 2\pi \xi_0 \xi_2 + \pi \sum_{n=1}^{\infty} (\xi_n \xi_{n+2} + \eta_n \eta_{n+2}) \right] . \tag{7.61}$$

Added to this is a similar expression for ψ_2 in terms of ϕ_i and χ_i, but with the change of integral limits to between k and 1 and without the σ^2 weighting. The **total denominator**, leaving out Δ^3 and higher terms, can be written

$$\sigma^2 \int_0^k s\, ds \left\{ (1 + 4\Delta^2 s^2)[2\pi \xi_0^2 + \pi \sum_{n=1}^{\infty} (\xi_n^2 + \eta_n^2)] + 4\Delta s \left[2\pi \xi_0 \xi_1 + \pi \sum_{n=1}^{\infty} (\xi_n \xi_{n+1} + \eta_n \eta_{n+1}) \right] \right.$$
$$\left. + 6\Delta^2 s^2 \left[\frac{\pi}{2} (\xi_1^2 - \eta_1^2) + 2\pi \xi_0 \xi_2 + \pi \sum_{n=1}^{\infty} (\xi_n \xi_{n+2} + \eta_n \eta_{n+2}) \right] \right\}$$
$$+ \int_k^1 s\, ds \, \{\text{a similar expression in } \phi_i \text{ and } \chi_i\} \,.$$

The numerator was given back at equation (7.45).

All the cross product terms are of the form $\xi_i \xi_j$, $\phi_i \phi_j$, $\eta_i \eta_j$ and $\chi_i \chi_j$. When $\Delta = 0$ these all disappear. There are no cross product terms of the form $\xi_i \eta_j$, $\phi_i \chi_j$ or $\xi_i \chi_j$, $\phi_i \eta_j$. This

demonstrates that there is separation between the even and odd modes of vibration and they can be stated separately. For the even modes of vibration all the terms with ξ and ϕ are utilized and η and χ are set $\eta = \chi = 0$. For the odd modes of vibration all the terms with η and χ are utilized and ξ and ϕ are set $\xi = \phi = 0$.

The even modes of vibration are therefore given by the following expression, if the sums of the cross-terms are written out explicitly:

$$\pi \int_0^k s\,ds \left\{ 2\xi_0'^2 + \sum_{n=1}^{\infty} (\xi_n'^2 + n^2\xi_n^2/s^2) \right\} + \pi \int_k^1 s\,ds \left\{ 2\phi_0'^2 + \sum_{n=1}^{\infty} (\phi_n'^2 + n^2\phi_n^2/s^2) \right\} \quad (7.62)$$

is the numerator of the expression and

$$\begin{aligned} \pi\sigma^2 \int_0^k s\,ds \{ & 2(1+4\Delta^2 s^2)\xi_0^2 + 2(4\Delta s)\xi_0\xi_1 + 2(6\Delta^2 s^2)\xi_0\xi_2 + (1+7\Delta^2 s^2)\xi_1^2 \\ & + (4\Delta s)\xi_1\xi_2 + (6\Delta^2 s^2)\xi_1\xi_3 + (1+4\Delta^2 s^2)\xi_2^2 + (4\Delta s)\xi_2\xi_3 + (6\Delta^2 s^2)\xi_2\xi_4 + ... \} \\ & + \pi \int_k^1 s\,ds \,\{\text{a similar expression in } \phi_i\} \end{aligned} \quad (7.63)$$

is the denominator.

The odd modes of vibration replace ξ_i and ϕ_i with η_i and χ_i in equations (7.62) and (7.63), although there are no η_0 and χ_0 terms and the $(1 + 7\Delta^2 s^2)$ coefficient that multiplys the ξ_1^2 and ϕ_1^2 terms in the denominator becomes $(1 + \Delta^2 s^2)$ when multiplying η_1^2 and χ_1^2.

With ψ_1 and ψ_2 written as Fourier series the boundary conditions (7.7), (7.8) and (7.9) become

$$\phi_n(1) = 0\,, \qquad \chi_n(1) = 0\,, \quad (7.64)$$

$$\xi_n(k) = \phi_n(k)\,, \qquad \eta_n(k) = \chi_n(k)\,, \quad (7.65)$$

$$\xi_n'(k) = \phi_n'(k)\,, \qquad \eta_n'(k) = \chi_n'(k) \quad (7.66)$$

with n=0,1,2... .

7.2 The Eigenfrequencies for the Concentric 2-Density Drum

The concentric case will now be investigated. This is the case where $\Delta = 0$, which relates to the 2-density case investigated by Ramakrishna and Sondhi [RS]. For this case there is no distinction between the even and odd modes of vibration so either ξ_n and ϕ_n or η_n and χ_n may be used. The cases $n = 0, 1, ...$ can be treated separately as s and θ are separable when $\Delta = 0$.

After using different trial functions for $\xi_n(s)$ and $\phi_n(s)$, Sarojini and Rahman found that the best results were related to the Taylor series of the Bessel function of the first kind (A.5). $\phi_n(s)$, which represents the Bessel fucntion of the second kind in the exact case, also has a logarithmic infinity. The functions used are:

for $n = 0$

$$\xi_0(s) = a_0^0 + a_2^0 s^2 + a_4^0 s^4 + a_0^0 s^6 \,, \tag{7.67}$$

$$\phi_0(s) = b_0^0 + b_2^0 s^2 + c_0^0 \log s \,; \tag{7.68}$$

for $n = 1$

$$\xi_1(s) = a_1^1 s + a_3^1 s^3 + a_5^1 s^5 \,, \tag{7.69}$$

$$\phi_1(s) = b_1^1 + b_3^1 s^3 + c_1^1 s \log s + c_3^1 s^3 \log s \,; \tag{7.70}$$

for $n = 2$

$$\xi_2(s) = a_2^2 s^2 + a_4^2 s^4 + a_6^2 s^6 + a_8^2 s^8 \,, \tag{7.71}$$

$$\phi_2(s) = b_2^2 s^2 + b_4^2 s^4 + c_2^2 s^2 \log s + c_4^2 s^4 \log s \,; \tag{7.72}$$

Looking at the $n = 0$ case, the 3 boundary conditions (7.7), (7.8) and (7.9) can be used to express 3 parameters from (7.67) and (7.68) in terms of the other parameters and k.

Using the boundary condition $\phi_0(1) = 0$, equation (7.68) becomes

$$\phi_0(1) = b_0^0 + b_2^0 1^2 + c_0^0 \log 1 \,, \tag{7.73}$$

which then simplifies to

$$0 = b_0^0 + b_2^0 \,. \tag{7.74}$$

This gives

$$\boxed{b_0^0 = -b_2^0 \,.} \tag{7.75}$$

Using equations (7.67) and (7.68) the boundary condition $\xi_0'(k) = \phi_0'(k)$ becomes

$$2a_2^0 k + 4a_4^0 k^3 + 6a_6^0 k^5 = 2b_2^0 k + \frac{c_0^0}{k} \,. \tag{7.76}$$

This gives c_0^0 as

$$\boxed{c_0^0 = \left(2a_2^0 k + 4a_4^0 k^3 + 6a_6^0 k^5 - 2b_2^0 k\right) k \,.} \tag{7.77}$$

Substituting (7.75) and (7.77) into equation (7.68), the boundary condition $\xi_0(k) = \phi_0(k)$ is written

$$a_0 + a_2^0 k^2 + a_4^0 k^4 + a_6^0 k^6 = -b_2^0 + b_2^0 k^2 + \left(2a_2^0 k + 4a_4^0 k^3 + 6a_6^0 k^5 - 2b_2^0 k\right) k \log k \,. \tag{7.78}$$

This gives a_0^0 as

$$\boxed{a_0^0 = -b_2^0 + b_2^0 k^2 + \left(2a_2^0 k + 4a_4^0 k^3 + 6a_6^0 k^5 - 2b_2^0 k\right) k \log k - a_2^0 k^2 - a_4^0 k^4 - a_6^0 k^6 \,.} \tag{7.79}$$

Equations (7.75), (7.77) and (7.79) are then substituted into (7.67) and (7.68), and then in turn into (7.33) and (7.34). As these are even modes of vibration the η_n and ξ_n terms are discarded and, for the case where $n = 0$, ψ_1 and ψ_2 are given by

$$\psi_1(s,\theta) = (-b_2^0 + b_2^0 k^2 + \left(2a_2^0 k + 4a_4^0 k^3 + 6a_6^0 k^5 - 2b_2^0 k\right) k \log k - a_2^0 k^2 \\ -a_4^0 k^4 - a_6^0 k^6 + a_2^0 s^2 + a_4^0 s^4 + a_0^0 s^6) \cos n\theta \,, \quad (7.80)$$

$$\psi_2(s,\theta) = -b_2^0 + b_2^0 s^2 + (2a_2^0 k + 4a_4^0 k^3 + 6a_6^0 k^5 - 2b_2^0 k) k \log s \,. \quad (7.81)$$

These expressions for ψ_1 and ψ_2 are then substituted into equation (7.31).

The system will exist in the lowest possible energy state allowed by the inital consitions and the functions used for $\xi_n(s)$ and $\phi_n(s)$. For an oscillator the lowest-energy system will be the system with the lowest frequency. The minimization of x will minimize the frequency of the vibration as $x = \lambda_2 b = \frac{\omega b}{c_2}$.

The right-hand side is minimized by using Maple 12 to vary the parameters a_2^0, a_4^0, a_6^0 and b_2^0. This gives the value of the lowest root for the concentric case where $n = 0$, $k = 0.4$, $\sigma = 3.125$ and $\Delta = 0$. This evaluates to give $x_{01} = 1.0068$.

The different solutions for x_{nj} must be orthogonal to one another. The equation that must hold for orthogonal solutions is given in the appendix of Ramakrishna and Sondhi's paper [RS] and, when a change of variables from r to s is made, is of the form

$$\int_0^k \int_0^{2\pi} \sigma^2 \, \psi_{1nj} \, \psi_{1n'j'} \, s \, ds \, d\theta + \int_k^1 \int_0^{2\pi} \psi_{2nj} \, \psi_{2n'j'} \, s \, ds \, d\theta = 0 \,. \quad (7.82)$$

This equation guarantees orthogonality when $n \neq n'$. This is because the θ integral evaluates to 0 for these cases as shown previously in equation (7.36). The equation is valid for the concentric case because the scale factor of the Laplacian is equal to 1.

To find x_{02}, equation (7.82) is used to restrict the values of the parameters. The values of the parameters that produced the minimum value of x are used to give ξ_0 and ϕ_0 for x_{01}:

$$\xi_{01}(s) = a_0^{01} + a_2^{01} s^2 + a_4^{01} s^4 + a_0^{01} s^6 \,, \quad (7.83)$$

$$\phi_{01}(s) = b_0^{01} + b_2^{01} s^2 + c_0^{01} \log s \,. \quad (7.84)$$

All the parameters are known from the minimization with $a_2^{01} = 3.3610$, $a_4^{01} = -4.3383$, $a_6^{01} = 10.091$ and $b_2^{01} = -0.088800$. The other parameters a_0^{01}, b_0^{01} and c_0^{01} are calculated from equations (7.75), (7.77) and (7.79).

ξ_0 and ϕ_0 for x_{02} are denoted

$$\xi_{02}(s) = a_0^{02} + a_2^{02} s^2 + a_4^{02} s^4 + a_0^{02} s^6 \,, \quad (7.85)$$

$$\phi_{02}(s) = b_0^{02} + b_2^{02} s^2 + c_0^{02} \log s \,, \quad (7.86)$$

and these equations, along with equations (7.33) and (7.34), and the found numerical parameters of ψ_1, are substituted into equation (7.82) and the equation is evaluated. b_2^{02}

is then given in terms of the ξ_{02} parameters as

$$b_2^{02} = -0.57748a_2^{02} - 0.17125a_4^{02} - 0.039508a_6^{02}\,. \tag{7.87}$$

The right-hand side of equation (7.31) is again minimized with this new restriction on b_2^{02} and x_{02} is found to be equal to 3.0799 .

The x_{03} root has to satisfy orthogonality with both the x_{02} and x_{01} roots. This reduces the free parameters for minimization to two, as the second orthogonality relation gives

$$a_2^{03} = -0.12266a_4^{03} - 0.011471a_6^{03}\,. \tag{7.88}$$

When the minimization is carried out x_{03} is found to be equal to 4.897 .

The same method is used to find the values of x_{11}, x_{12}, x_{21} and x_{22}. Due to the guaranteed orthogonality when $n \neq n'$, the minimization of the $j = 1$ functions can be implemented with only the boundary conditions satisfied, just like the x_{01} case.

For x_{31} the following functions were used:

$$\xi_3(s) = a_3^{31}s^3 + a_5^{31}s^5 + a_7^{31}s^7 + a_9^{31}s^9\,, \tag{7.89}$$

$$\phi_3(s) = b_3^{31}s^3 + b_5^{31}s^5 + c_3^{31}s^3\log s + c_5^{31}s^5\log s\,. \tag{7.90}$$

After minimization this produces the result $x_{31} = 3.9675$. An attempt was made to find a solution for x_{41} but Maple 12 could provide no evaluation with any accuracy or consistency for the trial functions that were used.

The resulted for the roots are divided by x_{01} to give the frequency ratios. The following table then compares them with the results from the previous method in Section 3 and the results found by Sarojini and Rahman [SR].

	Frequency ratio		
	Section 3	Saro. and Rahman	Maple 12 minimization
ψ_{01}	1.00	1.00	1.00
ψ_{11}	1.94	1.94	1.94
ψ_{21}	2.95	2.97	2.99
ψ_{02}	3.05	3.06	3.06
ψ_{31}	3.97	-	3.94
ψ_{12}	4.10	4.15	4.15
ψ_{03}	4.82	4.89	4.86
ψ_{22}	5.14	-	5.15

Table 7.1: Comparison of frequency ratios of harmonics with $\sigma = 3.125$ and $k = 0.4$, using the variational method

These results show that the variational method produces eigenfrequencies that have a high degree of accuracy in replicating the previously solved analytical model. The boundary conditions that are solved exactly by the 2-density model are solved numerically by this method, hence the method's effectiveness is determined by its agreement with the analytical solution. Unlike the method used in Section 3, this method can be extended to the asymmetric case to model the left-handed drum. Some alterations are needed before this

case can be solved. As $\Delta \neq 0$ for the asymmetric case, the cross product terms $\xi_i \xi_j$, where $i \neq j$, now remain in the denominator given by equation (7.63). Because of the presence of these terms, slight changes to the minimization method are required.

Chapter 8

Conclusion

This project has found the frequencies of the different modes of vibration belonging to three different drum models. The vibrational modes of the right-handed tabla have been found experimentally to have frequencies that are very close to perfect harmonicity (integer multiples of the fundamental frequency). The physical properties and construction techniques for the tabla were initially discussed, along with the work on vibrational modes by Sir C. V. Raman [IMD] and Ramakrishna and Sondhi [RS]. From this information, models for the tabla were created to replicate these vibrational modes.

The initial problem solved was that of the standard, one-density, drum. The frequency ratios of the vibrational modes of this model were found to have no apparent pattern. The project then focused on modelling the right-handed tabla. The simplest model for the right-handed tabla consists of two different concentric regions, each of constant density. The model was solved and the parameters were optimized, which then enabled the model to produce eigenfrequencies close to perfect harmonicity and in good agreement with the experimental values of the right-handed tabla (Table 3.1) .

The report then constructed a three-density model for the right-handed tabla, which produced eigenfrequency ratios in excellent agreement with the experimental values found by Ramakrishna and Sondhi (Table 5.3). The results produced by the 3-density model replicate the eigenfrequency ratios of the right-handed tabla more accurately than other existing models, including the results of recent numerical work [SA] [MS]. It is noted, however, that the precision of the parameters used to produce these results would be difficult to achieve in practice (Section 3.2.1) . The loaded region of the tabla is constructed with approximately seven layers and a model with even more density regions could better replicate this. This would provide better agreement with the experimental values and more stability in the parameters.

The next step of the project was to show that any damping within the membrane of the tabla would have a negligible affect on the frequency. This allowed the damping term to be excluded from the model.

A different method for solving the model was investigated that can also be used to solve the left-handed tabla. This method produced results that have a high degree of accuracy in replicating the previously solved analytical model.

Bibliography

[ARF] G. B. Arfken
Mathematical Methods for Physicists, 4th edition, Academic Press Inc., pg 628, ISBN 0-12-059815-9 (1995)

[B] D. J. Benson
Music: A Mathematical Offering, Cambridge University Press, Cambridge, IBSN 978-0-521-85387-3, (2007)

[BP] Wolfram Mathworld
`http://mathworld.wolfram.com/BipolarCoordinates.html`

[CT] *Crafting the Tabla*
`http://www.sadarang.com/Dhonkal.htm`

[CK] *The Syahi*
`http://chandrakantha.com/tablasite/articles/pudi4.htm`

[CKT] *Techniques*
`http://chandrakantha.com/tablasite/bsicbols.htm`

[FR] N. Fletcher, T. Rossing
The Physics of Musical Instruments, Springer-Verlag, New York, (1991)

[GGL] S. Gaudet, C. Gauthier and S. Léger
*Vibration of Indian Musical Drums, Journal of Sound and Vibration, **291**, 1-2, 388-394, (2006)*

[HT] V. E. Howle, L. N. Trefethen
*Eigenvalues of musical instruments, Journal of Computational and Applied Mathematics, **135**, 23-40, (2001)*

[K] A. Kapur
The Electronic Tabla, Computer Science Thesis, Princeton University, (2002)
`http://www.cs.princeton.edu/sound/research/controllers/etabla/Petthesis.pdf`

[IMD] Sir C V Raman,
*The Indian Musical Drums, Procedures of the Indian Academy of Sciences, **1A**, 179-188 (1934)*

[MS] S. S. Malu and A. Siddharthan
Acoustics of the Indian Drum, arXiv:math-ph/0001030v1, February 6, (2008)

[RS] B. S. Ramakrishna and M. M. Sondhi
Vibrations of Indian Musical Drums Regarded as Composite Membranes, Journal of the Acoustical Society of America, ***26****, 4, 523-529, (1954)*

[SA] G. Sathej and R. Adhikari
The eigenspectra of Indian musical drums, Journal of the Acoustical Society of America, ***2****, 831-838, (2009)*

[SR] T. Sarojin and A. Rahman
Variational Method for the Vibrations of the Indian Drums, Journal of the Acoustical Society of America, ***30****, 3, 191-196, (1958)*

[TT] *Tabla Tuning*,
`http://home.comcast.net/ tabla/tuningdetails.html`

Appendix A

Bessel Functions

Bessel functions are solutions of Bessel's Differential Equation, which is defined as:

$$x^2\frac{d^2y}{dx^2} + x\frac{dy}{dx} + (x^2 - n^2)y = 0\,. \tag{A.1}$$

Bessel functions discussed here have the common case where n is an integer. The general solution to this equation is

$$y(x) = a_1 J_n(x) + a_2 Y_n(x)\,, \tag{A.2}$$

where A and B are constants and $J_n(x)$ and $Y_n(x)$ are Bessel functions of the first and second kind respectively.

Bessel functions of the second kind have a singularity at $x = 0$. Therefore if the function has a finite value at $x = 0$ then $a_2 = 0$ and the Bessel function of the second kind can be ignored.

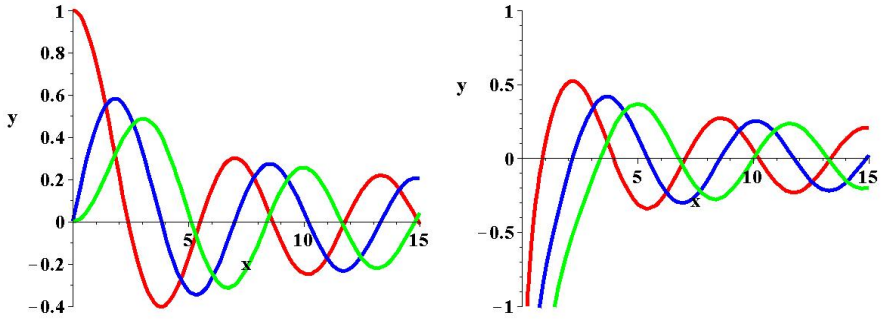

(a) $J_n(x)$ (b) $Y_n(x)$

Figure A.1: Bessel functions of the first and second kind for values of $n = 0$ (red), $n = 1$ (blue) and $n = 2$ (green)

A.1 Properties of Bessel functions

A.1.1 Identities

Bessel functions have the following properties:

$$\begin{aligned} J_{n+1}(x) &= \tfrac{2n}{x} J_n(x) - J_{n-1}(x)\,, \qquad & Y_{n+1}(x) &= \tfrac{2n}{x} Y_n(x) - Y_{n-1}(x)\,, \\ J'_n(x) &= \tfrac{1}{2}[J_{n-1}(x) - J_{n+1}(x)]\,, \qquad & Y'_n(x) &= \tfrac{1}{2}[Y_{n-1}(x) - Y_{n+1}(x)]\,. \end{aligned} \tag{A.3}$$

If the two equations of each kind are substituted into one another then the following two equations for each kind are produced:

$$\begin{aligned} J'_n(x) &= J_{n-1}(x) - \tfrac{n}{x} J_n(x)\,, \qquad & Y'_n(x) &= Y_{n-1}(x) - \tfrac{n}{x} Y_n(x)\,, \\ J'_n(x) &= \tfrac{n}{x} J_n(x) - J_{n+1}(x)\,, \qquad & Y'_n(x) &= \tfrac{n}{x} Y_n(x) - Y_{n+1}(x)\,. \end{aligned} \tag{A.4}$$

The Bessel function of the first kind can be defined by its Taylor Series expansion around $x = 0$, [ARF]:

$$J_n(x) = \sum_{s=0}^{\infty} \frac{(-1)^s}{s!\,(n+s)!} \Big(\frac{x}{2}\Big)^{n+2s}\,. \tag{A.5}$$

If $-n$ replaces n in this equation, and noting the fact that $(s-n)! \to \infty$ for $s = 0, ..., (n-1)$, the series can be started from $s = n$. It can then be seen that if n is negative then the following identity holds:

$$J_{-n}(x) = (-1)^n J_n(x)\,. \tag{A.6}$$

The Bessel function of the second kind can be defined in the following way:

$$Y_\nu(x) = \frac{J_\nu(x)\cos(\nu\pi) - J_{-\nu}(x)}{\sin(\nu\pi)}\,, \tag{A.7}$$

$$Y_n(x) = \lim_{\nu \to n} Y_\nu(x)\,, \tag{A.8}$$

where ν is a non-integer and n an integer. The non-integer Bessel function of the first kind subsititues ν for n and replaces the factorial term $(n+s)!$ with the gamma function $\Gamma(\nu + s + 1)$.

A.1.2 Bessel equation form with a solution of $J_n(\alpha x)$

If the equation to be solved is of the form

$$x_1^2 \frac{d^2 y}{dx_1^2} + x_1 \frac{dy}{dx_1} + (\alpha^2 x_1^2 - n^2) y = 0\,, \tag{A.9}$$

then it can be solved by the substitution of $x_1 = \frac{x_2}{\alpha}$. The chain rule $\frac{dy}{dx_1} = \frac{dy}{dx_2}\frac{dx_2}{dx_1} = \alpha\frac{dy}{dx_2}$ is used, along with $\frac{d^2y}{dx_1^2} = \frac{d}{dx_1}\left(\frac{dy}{dx_1}\right)$ and $\frac{d}{dx_1} = \frac{d}{dx_2}\frac{dx_2}{dx_1} = \alpha\frac{d}{dx_2}$.

This gives $\frac{d^2y}{dx_1^2} = \alpha^2\frac{d^2y}{dx_2^2}$, and the resulting equation is

$$x_2^2\frac{d^2y}{dx_2^2} + x_2\frac{dy}{dx_2} + (x_2^2 - n^2)y = 0\,.$$

Giving the general solution $\quad y(x_2) = a_1 J_n(x_2) + a_2 Y_n(x_2)\,, \quad$ or

$$\boxed{y(x_1) = a_1 J_n(\alpha x_1) + a_2 Y_n(\alpha x_1)\,.} \tag{A.10}$$

A.2 Bessel functions using Fourier theory

This section is outlined in Benson's 'Music: A Mathematical Offering' [B].

Fourier theory states that any periodic function can be written in the form

$$f(\theta) = \frac{1}{2}a_0 + \sum_{n=1}^{\infty}\left(a_n\cos(n\theta) + b_n\sin(n\theta)\right)\,, \tag{A.11}$$

where the coefficients are given by

$$a_n = \frac{1}{\pi}\int_{-\pi}^{\pi}\cos(n\theta)f(\theta)d\theta\,, \tag{A.12}$$

$$b_n = \frac{1}{\pi}\int_{-\pi}^{\pi}\sin(n\theta)f(\theta)d\theta\,. \tag{A.13}$$

Bessel functions can be thought of as the fourier series applied to $\sin(x\sin\theta)$ and $\cos(x\sin\theta)$.

The function $\sin(x\sin\theta)$ is odd: $\sin(x\sin\theta) = -\sin(x\sin(-\theta))$. This means its fourier coefficient a_n equals 0. It is also a half-period antisymmetric function: $\sin(x\sin\theta) = -\sin(x\sin(\theta-\pi))$. This gives the coefficients b_{2n} equal to zero, meaning only b_{2n+1} coefficients exist.

Now writing the general Fourier equation for $\sin(x\sin\theta)$ and using the Bessel function as the coefficient along with a factor of 2 to tidy the equation up later, the equation obtained is

$$\sin(x\sin\theta) = 2\sum_{n=0}^{\infty}J_{2n+1}(x)\sin((2n+1)\theta)\,. \tag{A.14}$$

The function $\cos(x\sin\theta)$ is even: $\cos(x\sin\theta) = \cos(x\sin(-\theta))$. This means its fourier coefficient b_n equals 0. It is also a half-period symmetric function: $\cos(x\sin\theta) = \cos(x\sin(\theta-\pi))$. This gives the coefficients a_{2n+1} equal to zero, meaning only a_{2n} coefficients exist.

Now writing the general Fourier equation for $\cos(x\sin\theta)$, as was done for the $\sin(x\sin\theta)$ case, gives:

$$\cos(x\sin\theta) = J_0(x) + 2\sum_{n=1}^{\infty} J_{2n}(x)\cos(2n\theta)\,. \tag{A.15}$$

Now the Bessel funciton is made the subject of the equation. Using the coefficient equation (A.13) and setting $b_n = 2J_{2n+1}(x)$ produces

$$2J_{2n+1}(x) = \frac{1}{\pi}\int_{-\pi}^{\pi} \sin((2n+1)\theta)\sin(x\sin\theta)d\theta\,. \tag{A.16}$$

Using the properties of an even function results in the equation

$$J_{2n+1}(x) = \frac{1}{\pi}\int_{0}^{\pi} \sin((2n+1)\theta)\sin(x\sin\theta)d\theta\,. \tag{A.17}$$

As seen while deriving equation (A.14) the function $\cos((2n+1)\theta)\cos(x\sin\theta)$ is half-period antisymmetric and has the value 0 at $\pi/2$, so

$$\frac{1}{\pi}\int_{0}^{\pi} \cos((2n+1)\theta)\cos(x\sin\theta)d\theta = 0\,. \tag{A.18}$$

Adding this to equation (A.16) gives

$$J_{2n+1} = \frac{1}{\pi}\int_{0}^{\pi} [\sin((2n+1)\theta)\sin(x\sin\theta) + \cos((2n+1)\theta)\cos(x\sin\theta)]d\theta\,. \tag{A.19}$$

Using the trigonometric identity $\cos(a-b) = \sin a\sin b + \cos a\cos b$, this can be simplified to

$$J_{2n+1} = \frac{1}{\pi}\int_{0}^{\pi} \cos\left((2n+1)\theta - z\sin\theta\right)d\theta\,. \tag{A.20}$$

Using a similar method for the a_n coefficient produces

$$J_{2n}(x) = \frac{1}{\pi}\int_{0}^{\pi} \cos(2n\theta - x\sin\theta)d\theta\,. \tag{A.21}$$

This gives use a common equation for both the odd and even integers and another definition for the Bessel function:

$$\boxed{J_n(x) = \frac{1}{\pi}\int_{0}^{\pi} \cos(n\theta - x\sin\theta)d\theta\,.} \tag{A.22}$$

Using the relation $J_{-n}(x) = (-1)^n J_n(x)$, in addition to the even and odd properties of $\sin(2n+1)\theta$ and $\cos(2n\theta)$, allows equations (A.12) and (A.13) to be written as sums from minus infinity to infinity as follows:

$$\sin(x\sin\theta) = \sum_{n=-\infty}^{\infty} J_{2n+1}(x)\sin((2n+1)\theta)\,, \tag{A.23}$$

$$\cos(x\sin\theta) = \sum_{n=-\infty}^{\infty} J_{2n}(x)\cos(2n\theta)\,. \tag{A.24}$$

Using the same properties and equation (A.21) again it can also be seen that $\sum_{n=-\infty}^{\infty} J_{2n}(x)\sin(2n\theta) = 0$ and $\sum_{n=-\infty}^{\infty} J_{2n+1}(x)\cos((2n+1)\theta) = 0$, leaving us able to simplify the equations as

$$\sin(x\sin\theta) = \sum_{n=-\infty}^{\infty} J_n(x)\sin(n\theta)\,, \tag{A.25}$$

$$\cos(x\sin\theta) = \sum_{n=-\infty}^{\infty} J_n(x)\cos(n\theta)\,. \tag{A.26}$$

A.2.1 Deriving the recurrance relations

Now the equations found in (A.3) for Bessel functions of the first kind can be derived. Starting with (A.25) it is differentiated with respect to θ giving

$$x\cos\theta\cos(x\sin\theta) = \sum_{n=-\infty}^{\infty} J_n(x)n\cos(n\theta)\,. \tag{A.27}$$

Now (A.26) is multiplied by $x\cos\theta$, producing

$$x\cos\theta\cos(x\sin\theta) = \sum_{n=-\infty}^{\infty} J_n(x)x\cos\theta\cos(n\theta)\,. \tag{A.28}$$

Then the trigonometric identity $\cos a\cos b = \frac{1}{2}(\cos(a+b)+\cos(a-b))$ is used on the right hand side to produce

$$x\cos\theta\cos(x\sin\theta) = \sum_{n=-\infty}^{\infty} J_n(x)\frac{x}{2}(\cos((n+1)\theta)+\cos((n-1)\theta))\,. \tag{A.29}$$

The equation can then be separated into two parts and reindexed, as the limits of the sum are $\pm\infty$ and the $\cos(n\theta)$ s are independent:

$$x\cos\theta\cos(x\sin\theta) = \sum_{n=-\infty}^{\infty} (J_{n-1}(x)+J_{n+1}(x))\frac{x}{2}\cos n\theta\,. \tag{A.30}$$

If equation (A.27) is now used to get the left hand side as $\sum_{n=-\infty}^{\infty} J_n(x)n\cos(n\theta)$, then, after rearranging, the produced relation is

$$\boxed{J_{n+1}(x) = \frac{2n}{x}J_n(x) - J_{n-1}(x)\,.} \tag{A.31}$$

To derive the other equation a similar method is used. Starting with (A.25), it is differentiated with respect to x:

$$\sin\theta\cos(x\sin\theta) = \sum_{n=-\infty}^{\infty} J_n'(x)\sin(n\theta)\,. \tag{A.32}$$

Now (A.25) is multiplied by $\sin\theta$ getting

$$\sin\theta\cos(x\sin\theta) = \sum_{n=-\infty}^{\infty} J_n(x)\sin\theta\cos(n\theta)\,. \tag{A.33}$$

Then the trigonometric identity $\sin a\cos b = \frac{1}{2}(\sin(a+b)+\sin(a-b))$ is used on the right hand side to produce, along with the odd property of sine, producing

$$\sin\theta\cos(x\sin\theta) = \sum_{n=-\infty}^{\infty} J_n(x)\frac{1}{2}(\sin((n+1)\theta)-\sin((n-1)\theta))\,. \tag{A.34}$$

The equation can then be separated into two parts and reindexed, as the limits of the sum are $\pm\infty$ and the $\sin(n\theta)$ s are independent, giving

$$\sin\theta\cos(x\sin\theta) = \sum_{n=-\infty}^{\infty} \frac{1}{2}(J_{n-1}(x)-J_{n+1}(x))\sin n\theta\,. \tag{A.35}$$

If equation (A.32) is now used to get the left hand side as $\sum_{n=-\infty}^{\infty} J_n'(x)\sin(n\theta)$. This is then rearranged to get the relation

$$\boxed{J_n'(x) = \frac{1}{2}(J_{n-1}(x)-J_{n+1}(x))\,.} \tag{A.36}$$

Appendix B

Bipolar Coordinates

Bipolar coordinates are a two-dimensional, orthogonal system of coordinates that creates two sets of circles on the two-dimensional plane.

B.1 Properties of Bipolar Coordinates

The bipolar coordinate system is defined by the transformation equations [BP]. The foci are located at $\pm\alpha$ (see Figure B.1).

The transformation equations are

$$x = \frac{\alpha \sinh \xi}{\cosh \xi - \cos \theta}\,, \qquad\qquad y = \frac{\alpha \sin\ \theta}{\cosh \xi - \cos \theta}\,. \tag{B.1}$$

Circles are produced when θ is constant of the form

$$x^2 + (y - \alpha \cot \theta)^2 = \frac{\alpha^2}{\sin^2 \theta}\,, \tag{B.2}$$

and when ξ is constant circles are produced of the form

$$y^2 + (x - \alpha \coth \xi)^2 = \frac{\alpha^2}{\sinh^2 \xi}\,. \tag{B.3}$$

The scale factor is given by the equation

$$h_\xi = h_\theta = \frac{\alpha}{\cosh \xi - \cos \theta}\,. \tag{B.4}$$

The blue circles in Figure B.1 are the circles of constant ξ and the red circles are the circles of constant θ. The asymmetric drum in the bipolar coordinate system is represented by

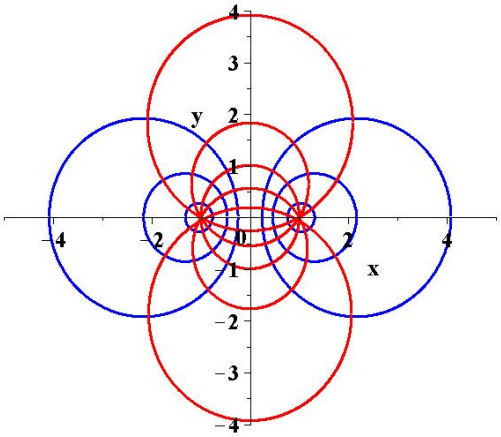

Figure B.1: Bipolar coordinates with the foci located at (-1,0) and (1,0)

two of the circles of constant ξ, one within the other. The outer circle represents the edge of the drum membrane and the inner circle the loaded region. The circles of constant θ are then the equivalent of radial lines in normal polar coordinates.

B.2 Finding the Circle Equations

To have Bipolar coordinates two different sets of circles must exist. One set when θ is constant and one set when ξ is constant.

First the circle of constant θ will be derived. If the x equation from (B.1) is divided by the y equation, it gives

$$\boxed{\frac{x}{y} = \frac{\sinh\xi}{\sin\theta}\,.} \tag{B.5}$$

Using $\sinh\xi = \pm\sqrt{\cosh^2\xi - 1}$ this can also be written

$$\frac{x}{y} = \frac{\pm\sqrt{\cosh^2\xi - 1}}{\sin\theta}\,. \tag{B.6}$$

Multiplying both sides by $\sin\theta$ produces

$$\pm\sqrt{\cosh^2\xi - 1} = \frac{x}{y}\sin\theta\,.$$

This is rearranged to make $\cosh\xi$ the subject, which gives

$$\cosh\xi = \pm\sqrt{\frac{x^2}{y^2}\sin^2\theta + 1}\,. \tag{B.7}$$

This is then substituted into the y equation (B.1) to give y as a function of one variable:

$$y = \frac{\alpha \sin\theta}{\pm\sqrt{\frac{x^2}{y^2}\sin^2\theta + 1} - \cos\theta}\,. \tag{B.8}$$

To show this can satisfy a circle equation of the form
$(x-a)^2 + (y-b)^2 = r^2$ it must be rearranged in the following manner:

$$\left(\pm\sqrt{\frac{x^2}{y^2}\sin^2\theta + 1} - \cos\theta\right) y = \alpha\sin\theta\,. \tag{B.9}$$

Both sides are then divided by y and the $\cos\theta$ is moved across the equality giving

$$\pm\sqrt{\frac{x^2}{y^2}\sin^2\theta + 1} = \frac{\alpha}{y}\sin\theta + \cos\theta\,. \tag{B.10}$$

Squaring both sides then produces

$$\frac{x^2}{y^2}\sin^2\theta + 1 = \frac{\alpha^2}{y^2}\sin^2\theta + \frac{2\alpha}{y}\sin\theta\cos\theta + \cos^2\theta\,. \tag{B.11}$$

Both sides are next multiplyied by $\frac{y^2}{\sin^2\theta}$ to give

$$x^2 + \frac{y^2}{\sin^2\theta} = \alpha^2 + 2\alpha y\frac{\cos\theta}{\sin\theta} + y^2\frac{\cos^2\theta}{\sin^2\theta}\,, \tag{B.12}$$

and are rearranged, resulting in

$$x^2 + y^2\left(\frac{1-\cos^2\theta}{\sin^2\theta}\right) - 2\alpha y\frac{\cos\theta}{\sin\theta} - \alpha^2 = 0\,. \tag{B.13}$$

Using $1-\cos^2\theta = \sin^2\theta$ and $\frac{1-\cos^2\theta}{\sin^2\theta} = 1$ now gives

$$x^2 + y^2 - 2\alpha y\frac{\cos\theta}{\sin\theta} - \alpha^2\frac{1-\cos^2\theta}{\sin^2\theta} = 0\,. \tag{B.14}$$

Factorizing this gives the circle equation when θ is constant, which has the form

$$\boxed{x^2 + \left(y - \frac{\alpha}{\tan\theta}\right)^2 = \frac{\alpha^2}{\sin^2\theta}\,.} \tag{B.15}$$

If θ is constant then circles are produced as shown in Figure B.2 .

The same method is used to find the circles of constant ξ. Starting with equation (B.5) and using $\sin\theta = \sqrt{1-\cos^2\theta}$ gives

$$\frac{x^2}{y^2} = \frac{\sinh^2\xi}{1-\cos^2\theta}\,. \tag{B.16}$$

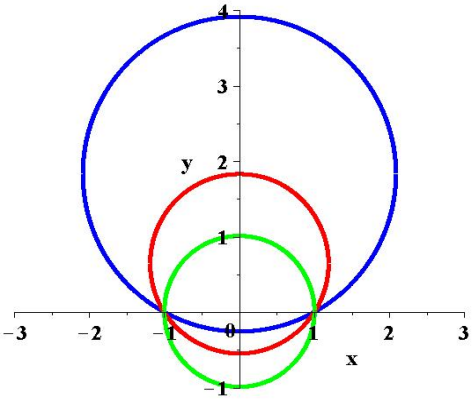

Figure B.2: Circles of constant θ with the foci located at (-1,0) and (1,0) for values of $\theta = 0.5$ (blue), $\theta = 1$ (red) and $\theta = 1.5$ (green)

This is rearranged to get

$$\cos\theta = \sqrt{1 - \frac{y^2}{x^2}\sinh^2\xi}\,, \tag{B.17}$$

and substituted into the x equation from (B.1) to give x as a function of ξ:

$$x = \frac{\alpha\sinh\xi}{\cosh\xi - \sqrt{1 - \frac{y^2}{x^2}\sinh^2\xi}}\,. \tag{B.18}$$

Through rearranging this can become

$$1 - \frac{y^2}{x^2}\sinh^2\xi = \left(\cosh\xi - \frac{\alpha}{x}\sinh\xi\right)^2\,. \tag{B.19}$$

Multiplying out the bracket produces

$$1 - \frac{y^2}{x^2}\sinh^2\xi = \cosh^2\xi - \frac{2\alpha}{x}\cosh\xi\sinh\xi + \frac{\alpha^2}{x^2}\sinh^2\xi\,. \tag{B.20}$$

Multiplying both sides by $\frac{x^2}{\sinh^2\xi}$ results in the equation

$$\frac{x^2}{\sinh^2\xi} - y^2 = x^2\frac{\cosh^2\xi}{\sinh^2\xi} - 2\alpha x\frac{\cosh\xi}{\sinh\xi} + \alpha^2\,. \tag{B.21}$$

After grouping the terms together the equation becomes

$$x^2\frac{\cosh^2\xi - 1}{\sinh^2\xi} - 2\alpha x\frac{\cosh\xi}{\sinh\xi} + \alpha^2 + y^2 = 0\,. \tag{B.22}$$

Factorizing gives the circle equation for constant ξ:

$$\boxed{\left(x - \alpha\frac{\cosh\xi}{\sinh\xi}\right)^2 + y^2 = \frac{\alpha^2}{\sinh^2\xi}\,.} \tag{B.23}$$

When ξ is constant the circles produced will be located as shown in Figure B.3 .

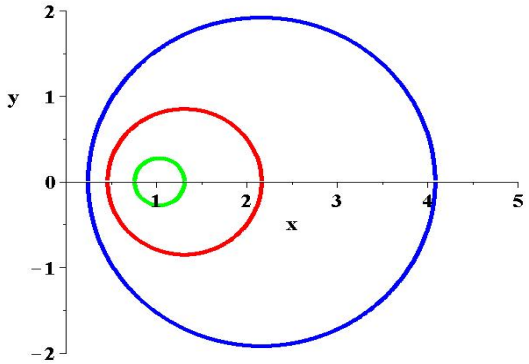

Figure B.3: Circles of constant ξ with the focus located at (1,0) for values of $\xi = 0.5$ (blue), $\xi = 1$ (red)and $\xi = 2$ (green)

B.3 Deriving the Bipolar Scale Factor

The simplist way to obtain the scale factor is through the line element, using the equation

$$(ds)^2 = (dx)^2 + (dy)^2 = h_\xi (d\xi)^2 + h_\theta (d\theta)^2 \,. \tag{B.24}$$

Differentiating x from equation (B.1) produces

$$dx = \alpha \left(\frac{\cosh \xi}{\cosh \xi - \cos \theta} + \frac{-\sinh^2 \xi}{(\cosh \xi - \cos \theta)^2} \right) d\xi - \frac{\alpha \sinh \xi \sin \theta}{(\cosh \xi - \cos \theta)^2} d\theta \,. \tag{B.25}$$

The $d\xi$ terms are grouped together as one fraction giving

$$dx = \alpha \frac{\cosh^2 \xi - \cos \theta \cosh \xi - \sinh^2 \xi}{(\cosh \xi - \cos \theta)^2} d\xi - \frac{\alpha \sinh \xi \sin \theta}{(\cosh \xi - \cos \theta)^2} d\theta \,. \tag{B.26}$$

Using the identity $\cosh^2 x - \sinh^2 x = 1$ this becomes

$$\boxed{dx = \alpha \frac{1 - \cos \theta \cosh \xi}{(\cosh \xi - \cos \theta)^2} d\xi - \frac{a \sinh \xi \sin \theta}{(\cosh \xi - \cos \theta)^2} d\theta \,.} \tag{B.27}$$

Similarly, differentiating y from equation (B.1) gives

$$dy = \alpha \frac{-\sin \theta \sinh \xi}{(\cosh \xi - \cos \theta)^2} d\xi + \alpha \left(\frac{\cos \theta}{\cosh \xi - \cos \theta} + \frac{-\sin^2 \theta}{(\cosh \xi - \cos \theta)^2} \right) d\theta \,, \tag{B.28}$$

and when the $d\theta$ terms are written in the same fraction gives

$$dy = \alpha \frac{-\sin \theta \sinh \xi}{(\cosh \xi - \cos \theta)^2} d\xi + \alpha \frac{\cosh \xi \cos \theta - \cos^2 \theta - \sin^2 \theta}{(\cosh \xi - \cos \theta)^2} d\theta \,. \tag{B.29}$$

Using the identity $\cos^2 x + \sin^2 x = 1$, the next step is

$$\boxed{dy = \alpha \frac{-\sin\theta \sinh\xi}{(\cosh\xi - \cos\theta)^2} d\xi + \alpha \frac{\cosh\xi\cos\theta - 1}{(\cosh\xi - \cos\theta)^2} d\theta\,.} \tag{B.30}$$

Now, if (B.27) and (B.30) are squared and added together then they produce

$$\begin{aligned}(dx)^2 + (dy)^2 = \alpha^2 &\left(\left(\frac{1 - \cos\theta\cosh\xi}{(\cosh\xi - \cos\theta)^2} \right)^2 + \left(\frac{\sin\theta\sinh\xi}{(\cosh\xi - \cos\theta)^2} \right)^2 \right) (d\xi)^2 \\ &+\alpha^2 \left(\left(\frac{\sinh\xi\sin\theta}{(\cosh\xi - \cos\theta)^2} \right)^2 + \left(\frac{\cosh\xi\cos\theta - 1}{(\cosh\xi - \cos\theta)^2} \right)^2 \right) (d\theta)^2 + f(\xi,\theta) d\xi d\theta\,,\end{aligned} \tag{B.31}$$

where $f(\xi,\theta)d\xi d\theta$ is the crossterm from squaring dx and squaring dy. If a common denominator is found for the terms of each integral then the equation formed is

$$\begin{aligned}(dx)^2 + (dy)^2 = \alpha^2 &\frac{1 - 2\cos\theta\cosh\xi + \cos^2\theta\cosh^2\xi + \sin^2\theta\sinh^2\xi}{(\cosh\xi - \cos\theta)^4} (d\xi)^2 \\ &+\alpha^2 \frac{\sinh^2\xi\sin^2\theta + \cosh^2\xi\cos^2\theta - 2\cosh\xi\cos\theta + 1}{(\cosh\xi - \cos\theta)^4} (d\theta)^2 + f(\xi,\theta) d\xi d\theta\,.\end{aligned} \tag{B.32}$$

Using the substitution $\sin^2\theta = 1 - \cos^2\theta$, gives

$$\begin{aligned}(dx)^2 + (dy)^2 = \alpha^2 &\frac{1 - 2\cos\theta\cosh\xi + \cos^2\theta\cosh^2\xi + (1 - \cos^2\theta)\sinh^2\xi}{(\cosh\xi - \cos\theta)^4} (d\xi)^2 \\ &+\alpha^2 \frac{\sinh^2\xi(1 - \cos^2\theta) + \cosh^2\xi\cos^2\theta - 2\cosh\xi\cos\theta + 1}{(\cosh\xi - \cos\theta)^4} (d\theta)^2 + f(\xi,\theta) d\xi d\theta\,.\end{aligned} \tag{B.33}$$

Now using $\cosh^2\theta - \sinh^2\theta = 1$, produces

$$\begin{aligned}(dx)^2 + (dy)^2 = \alpha^2 &\frac{1 - 2\cos\theta\cosh\xi + \cosh^2\xi - 1 + \cos^2}{(\cosh^2\xi - 2\cosh\xi\cos\theta + \cos^2\theta)^2} (d\xi)^2 \\ &+\alpha^2 \frac{1 + \cos^2\theta + \cosh^2\xi - 2\cos\theta\cosh\xi - 1}{(\cosh^2\xi - 2\cosh\xi\cos\theta + \cos^2\theta)^2} (d\theta)^2 + f(\xi,\theta) d\xi d\theta\,.\end{aligned} \tag{B.34}$$

Both numerators cancel out with a factor of the denominator leaving us with the same result for both scale factors:

$$(dx)^2 + (dy)^2 = \frac{\alpha^2}{\cosh^2\xi - 2\cosh\xi\cos\theta + \cos^2\theta} \left[(d\xi)^2 + (d\theta)^2 \right] + f(\xi,\theta) d\xi d\theta\,, \tag{B.35}$$

or

$$(dx)^2 + (dy)^2 = \frac{\alpha^2}{(\cosh\xi - \cos\theta)^2} \left[(d\xi)^2 + (d\theta)^2 \right] + f(\xi,\theta) d\xi d\theta\,. \tag{B.36}$$

The cross-terms produced in (B.31) are

$$f(\xi,\theta)d\xi d\theta = 2\alpha\frac{(1-\cos\theta\cosh\xi)(-\sinh\xi\sin\theta)}{(\cosh\xi-\cos\theta)^2}d\xi d\theta + 2\alpha\frac{(-\sinh\xi\sin\theta)(\cos\theta\cosh\xi-1)}{(\cosh\xi-\cos\theta)^2}d\xi d\theta\,. \tag{B.37}$$

From the numerators it can be seen that the cross-terms cancel out leaving

$$f(\xi,\theta)d\xi d\theta = 0\,. \tag{B.38}$$

An orthogonal basis has been obtained with scale factors equal to

$$h_\xi^2 = h_\theta^2 = \frac{\alpha^2}{(\cosh\xi-\cos\theta)^2}\,. \tag{B.39}$$

The squares then cancel to give

$$\boxed{h_\xi = h_\theta = \frac{\alpha}{\cosh\xi-\cos\theta}\,.} \tag{B.40}$$

B.4 Modified Bipolar Coordinates

Sarojini and Rahman use a modified bipolar coordinate system in their work on the asymmetric Indian Drum [SR]. This gives a set of concentric circles if r is constant and α and $(\alpha - z)$ approaches infinity. This is analagous to the right-handed drum with r and θ ordinary polar coordinates. The transform is given by

$$r = 2\alpha e^{\xi}\,, \tag{B.41}$$

or

$$\xi = \ln\frac{r}{2\alpha}\,. \tag{B.42}$$

Substituted in to the cartesian orthodox bipolar transforms in equations (B.1) produces

$$x = \alpha\frac{\frac{r}{4\alpha}-\frac{\alpha}{r}}{\frac{r}{4\alpha}+\frac{\alpha}{r}-\cos\theta}\,, \qquad y = \alpha\frac{\sin\ \theta}{\frac{r}{4\alpha}+\frac{\alpha}{r}-\cos\theta}\,. \tag{B.43}$$

If this is multiplied by $\frac{4\alpha r}{4\alpha r}$ it tidies up to

$$\boxed{x = \frac{r^2-4\alpha^2}{r^2+4\alpha^2-4\alpha r\cos\theta}\,,} \qquad \boxed{y = \frac{4\alpha r\sin\ \theta}{r^2+4\alpha^2-4\alpha r\cos\theta}\,.} \tag{B.44}$$

The scale factor is modified by the change in variable. The Laplacian of unmodified bipolar coordinates is given by

$$\nabla^2 = \frac{1}{h^2}\left(\frac{\partial^2}{\partial\xi^2}+\frac{\partial^2}{\partial\theta^2}\right)\,. \tag{B.45}$$

Now a substitution must be made for the ξ differential. Equation (B.41) is used to get

$$\frac{\partial}{\partial \xi} = \frac{\partial r}{\partial \xi}\frac{\partial}{\partial r} = r\frac{\partial}{\partial r}\,. \tag{B.46}$$

Using the chain rule

$$\frac{\partial^2}{\partial \xi^2} = \frac{\partial}{\partial \xi}\left(r\frac{\partial}{\partial r}\right) = \frac{\partial r}{\partial \xi}\frac{\partial}{\partial r}\left(r\frac{\partial}{\partial r}\right)\,, \tag{B.47}$$

$$\frac{\partial^2}{\partial \xi^2} = r\frac{\partial}{\partial r} + r^2\frac{\partial^2}{\partial r^2}\,. \tag{B.48}$$

The Laplacian is now

$$\nabla^2 = \frac{1}{h^2}\left(r^2\frac{\partial^2}{\partial r^2} + r\frac{\partial}{\partial r} + \frac{\partial^2}{\partial \theta^2}\right)\,, \tag{B.49}$$

or

$$\nabla^2 = \frac{r^2}{h^2}\left(\frac{\partial^2}{\partial r^2} + \frac{1}{r}\frac{\partial}{\partial r} + \frac{1}{r^2}\frac{\partial^2}{\partial \theta^2}\right)\,, \tag{B.50}$$

which gives the ordinary polar coordinates Laplacian as the bracket with a scale factor. If equation (B.40) is substituted into (B.50) the result is

$$\nabla^2 = \frac{\left(\frac{r}{4\alpha} + \frac{\alpha}{r} - \cos\theta\right)^2}{\alpha^2} r^2\left(\frac{\partial^2}{\partial r^2} + \frac{1}{r}\frac{\partial}{\partial r} + \frac{1}{r^2}\frac{\partial^2}{\partial \theta^2}\right)\,. \tag{B.51}$$

When used with polar coordinate identities this gives a modified bipolar coordinate scale factor of

$$\boxed{h = \frac{\alpha}{\frac{r^2}{4\alpha} + \alpha - r\cos\theta}\,.} \tag{B.52}$$

Appendix C

Maple Programs

Included here are the Maple 12 programs used to solve the eigenvalue equation, draw the graphs and optimize the parameters for minimum error. The limits within which the different harmonics are searched for in the optimization programmes need to be altered if the 1-density case is solved.

C.1 Solution and Graphs of the 2-Density Drum

Setting the parameters
> n := 0; sigma := 2.84; a := .385; b := 1; k := a/b; Amp := 1;

The 2-density eigenvalue equation
> c := sigma*BesselJ(n-1, sigma*k*x)/BesselJ(n, sigma*k*x)-(BesselY(n, x)*BesselJ(n-1, k*x)-BesselJ(n, x)*BesselY(n-1, k*x))/(BesselY(n, x)*BesselJ(n, k*x)-BesselJ(n, x)*BesselY(n, k*x));

Plot equation to locate roots
> plot(c, x = 0 .. 13, -100 .. 100);

Solve equation for chosen root
> d := fsolve(c = 0, x = 1 .. 2);

Radial plot of outer region
> e := Amp*BesselJ(n, sigma*k*d)*(BesselY(n, d)*BesselJ(n, d*r/b)-BesselJ(n, d)*BesselY(n, d*r/b))/(BesselY(n, d)*BesselJ(n, k*d)-BesselJ(n, d)*BesselY(n, k*d));
> plot(e, r = 0 .. b, -1 .. 5);

Radial plot of inner region

> f := Amp*BesselJ(n, sigma*k*d*r/a);
> plot(f, r = 0 .. b, -1 .. 5);

Radial plot of drum membrane
> g := plot(e, r = a .. b, -1 .. 1); h := plot(f, r = 0 .. a, -1 .. 1); with(plots);
> display(g, h);

3D plot of drum membrane
> i := plot3d([r, theta, e*cos(n*theta)], r = a .. b, theta = 0 .. 2*Pi, coords = cylindrical);
l := plot3d([r, theta, f*cos(n*theta)], r = 0 .. a, theta = 0 .. 2*Pi, coords = cylindrical, colour=black); m := plot3d([r, theta, f*cos(n*theta)], r = 0 .. a, theta = 0 .. 2*Pi, coords = cylindrical, style=wireframe,colour=grey);
> display(i, l, m);

C.2 Optimizing the 2-Density Parameters

Error calculation
> Error4 := **proc** (sigma, k) **local** x01, x02, x03, x11, x12, x13, x21, x22, x31, x41;
x01 := fsolve(sigma*BesselJ(-1, sigma*k*y)/BesselJ(0, sigma*k*y)-(BesselY(0, y)*BesselJ(-1, k*y)-BesselJ(0, y)*BesselY(-1, k*y))/(BesselY(0, y)*BesselJ(0, k*y)-BesselJ(0, y)*BesselY(0, k*y)) = 0);
x02 := fsolve(sigma*BesselJ(-1, sigma*k*y)/BesselJ(0, sigma*k*y)-(BesselY(0, y)*BesselJ(-1, k*y)-BesselJ(0, y)*BesselY(-1, k*y))/(BesselY(0, y)*BesselJ(0, k*y)-BesselJ(0, y)*BesselY(0, k*y)) = 0, y = 2*x01 .. 4*x01);
x03 := fsolve(sigma*BesselJ(-1, sigma*k*y)/BesselJ(0, sigma*k*y)-(BesselY(0, y)*BesselJ(-1, k*y)-BesselJ(0, y)*BesselY(-1, k*y))/(BesselY(0, y)*BesselJ(0, k*y)-BesselJ(0, y)*BesselY(0, k*y)) = 0, y = 5*x01 .. 7*x01);
x11 := fsolve(sigma*BesselJ(0, sigma*k*y)/BesselJ(1, sigma*k*y)-(BesselY(1, y)*BesselJ(0, k*y)-BesselJ(1, y)*BesselY(0, k*y))/(BesselY(1, y)*BesselJ(1, k*y)-BesselJ(1, y)*BesselY(1, k*y)) = 0, y = x01 .. 3*x01);
x12 := fsolve(sigma*BesselJ(0, sigma*k*y)/BesselJ(1, sigma*k*y)-(BesselY(1, y)*BesselJ(0, k*y)-BesselJ(1, y)*BesselY(0, k*y))/(BesselY(1, y)*BesselJ(1, k*y)-BesselJ(1, y)*BesselY(1, k*y)) = 0, y = 3*x01 .. 5*x01);
x13 := fsolve(sigma*BesselJ(0, sigma*k*y)/BesselJ(1, sigma*k*y)-(BesselY(1, y)*BesselJ(0, k*y)-BesselJ(1, y)*BesselY(0, k*y))/(BesselY(1, y)*BesselJ(1, k*y)-BesselJ(1, y)*BesselY(1, k*y)) = 0, y = 4*x01 .. 6*x01);
x21 := fsolve(sigma*BesselJ(1, sigma*k*y)/BesselJ(2, sigma*k*y)-(BesselY(2, y)*BesselJ(1, k*y)-BesselJ(2, y)*BesselY(1, k*y))/(BesselY(2, y)*BesselJ(2, k*y)-BesselJ(2, y)*BesselY(2, k*y)) = 0, y = 2*x01 .. 4*x01);
x22 := fsolve(sigma*BesselJ(1, sigma*k*y)/BesselJ(2, sigma*k*y)-(BesselY(2, y)*BesselJ(1, k*y)-BesselJ(2, y)*BesselY(1, k*y))/(BesselY(2, y)*BesselJ(2, k*y)-BesselJ(2, y)*BesselY(2, k*y)) = 0, y = 4*x01 .. 6*x01);
x31 := fsolve(sigma*BesselJ(2, sigma*k*y)/BesselJ(3, sigma*k*y)-(BesselY(3, y)*BesselJ(2, k*y)-BesselJ(3, y)*BesselY(2, k*y))/(BesselY(3, y)*BesselJ(3, k*y)-BesselJ(3, y)*BesselY(3, k*y)) = 0, y = 3*x01 .. 5*x01);

x41 := fsolve(sigma*BesselJ(3, sigma*k*y)/BesselJ(4, sigma*k*y)-(BesselY(4, y)*BesselJ(3, k*y)-BesselJ(4, y)*BesselY(3, k*y))/(BesselY(4, y)*BesselJ(4, k*y)-BesselJ(4, y)*BesselY(4, k*y)) = 0, y = 4*x01 .. 6*x01); **return** (1/9)*(x02/x01-3)^2+(1/4)*(x11/x01-2)^2+(1/16)*(x12/x01-4)^2+(1/25)*(x13/x01-5)^2+(1/9)*(x21/x01-3)^2+(1/25)*(x22/x01-5)^2+(1/16)*(x31/x01-4)^2+(1/25)*(x41/x01-5)^2 **end proc**;

Parameter input
> Error4(2.84, .385);

C.3 Optimizing the 3-Density Parameters

Parameter input
> (sigmaValues, tauValues, kValues, qValues) := ({1.04, 1.05, 1.06}, {2.81, 2.82, 2.83}, {.37, .38, .39}, {.38, .39, .40});

Producing every permutation of parameters
> V := combinat[cartprod]([‘sigma;Values‘, ‘tau;Values‘, kValues, qValues]);
> T := table();
> for i while not V[finished] do T[i] := V[nextvalue]() end do;
> comb := [seq(T[j], j = 1 .. i-1)];

Error calculation
> Err1 := **proc** (sigma, tau, k, q) **local** x01, x02, x03, x11, x12, x13, x21, x22, x31, x41, beta, beta1, beta2, beta3, beta4, TheError;
beta := (BesselY(-1, sigma*k*q*y)*BesselJ(0, sigma*tau*k*q*y)-tau*BesselJ(-1, sigma*tau*k*q*y)*BesselY(0, sigma*k*q*y))/(tau*BesselJ(-1, sigma*tau*k*q*y)*BesselJ(0, sigma*k*q*y)-BesselJ(-1, sigma*k*q*y)*BesselJ(0, sigma*tau*k*q*y));
beta1 := (BesselY(0, sigma*k*q*y)*BesselJ(1, sigma*tau*k*q*y)-tau*BesselJ(0, sigma*tau*k*q*y)*BesselY(1, sigma*k*q*y))/(tau*BesselJ(0, sigma*tau*k*q*y)*BesselJ(1, sigma*k*q*y)-BesselJ(0, sigma*k*q*y)*BesselJ(1, sigma*tau*k*q*y));
beta2 := (BesselY(1, tau*k*q*y)*BesselJ(2, sigma*tau*k*q*y)-tau*BesselJ(1, sigma*tau*k*q*y)*BesselY(2, sigma*k*q*y))/(tau*BesselJ(1, sigma*tau*k*q*y)*BesselJ(2, tau*k*q*y)-BesselJ(1, sigma*k*q*y)*BesselJ(2, sigma*tau*k*q*y));
beta3 := (BesselY(2, sigma*k*q*y)*BesselJ(3, sigma*tau*k*q*y)-tau*BesselJ(2, sigma*tau*k*q*y)*BesselY(3, sigma*k*q*y))/(tau*BesselJ(2, sigma*tau*k*q*y)*BesselJ(3, sigma*k*q*y)-BesselJ(2, sigma*k*q*y)*BesselJ(3, sigma*tau*k*q*y));
beta4 := (BesselY(3, sigma*k*q*y)*BesselJ(4, sigma*tau*k*q*y)-tau*BesselJ(3, sigma*tau*k*q*y)*BesselY(4, sigma*k*q*y))/(tau*BesselJ(3, sigma*tau*k*q*y)*BesselJ(4, sigma*k*q*y)-BesselJ(3, sigma*k*q*y)*BesselJ(4, sigma*tau*k*q*y));
x01 := fsolve(sigma*(beta*BesselJ(-1, sigma*k*y)+BesselY(-1, sigma*k*y))/(beta*BesselJ(0, sigma*k*y)+BesselY(0, sigma*k*y))-(BesselY(0, y)*BesselJ(-1, k*y)-BesselJ(0, y)*BesselY(-1, k*y))/ (BesselY(0, y)*BesselJ(0, k*y)-BesselJ(0, y)*BesselY(0, k*y)), y = 0 .. 2);
x02 := fsolve(sigma*(beta*BesselJ(-1, sigma*k*y)+BesselY(-1, sigma*k*y))/(beta*BesselJ(0, sigma*k*y)+ BesselY(0, sigma*k*y))-(BesselY(0, y)*BesselJ(-1, k*y)-BesselJ(0, y)*BesselY(-1,k*y))/(BesselY(0,y)*BesselJ(0, k*y)-BesselJ(0,y)*BesselY(0,k*y)), y = 2*x01 ..4*x01);

x03 := fsolve(sigma*(beta*BesselJ(-1, sigma*k*y)+BesselY(-1, sigma*k*y))/(beta*BesselJ(0, sigma*k*y)+BesselY(0, sigma*k*y))-(BesselY(0, y)*BesselJ(-1,k*y)-BesselJ(0,y)*BesselY(-1,k*y))/ (BesselY(0,y)*BesselJ(0,k*y)-BesselJ(0,y)*BesselY(0,k*y)), y=4.5*x01 ..5.5*x01);
x11 := fsolve(sigma*(beta1*BesselJ(0, sigma*k*y)+BesselY(0, sigma*k*y))/(beta1*BesselJ(1, sigma*k*y)+BesselY(1, sigma*k*y))-(BesselY(1, y)*BesselJ(0, k*y)-BesselJ(1, y)*BesselY(0, k*y))/(BesselY(1, y)*BesselJ(1, k*y)-BesselJ(1, y)*BesselY(1, k*y)), y = x01 .. 3*x01);
x12 := fsolve(sigma*(beta1*BesselJ(0, sigma*k*y)+BesselY(0, sigma*k*y))/(beta1*BesselJ(1, sigma*k*y)+BesselY(1, sigma*k*y))-(BesselY(1, y)*BesselJ(0, k*y)-BesselJ(1, y)*BesselY(0, k*y))/ (BesselY(1, y)*BesselJ(1, k*y)-BesselJ(1, y)*BesselY(1, k*y)), y = 3*x01 .. 5*x01);
x13 := fsolve(sigma*(beta1*BesselJ(0, sigma*k*y)+BesselY(0, sigma*k*y))/(beta1*BesselJ(1, sigma*k*y)+BesselY(1, sigma*k*y))-(BesselY(1, y)*BesselJ(0, k*y)-BesselJ(1, y)*BesselY(0, k*y))/ (BesselY(1, y)*BesselJ(1, k*y)-BesselJ(1, y)*BesselY(1, k*y)), y = 4*x01 .. 6*x01);
x21 := fsolve(sigma*(beta2*BesselJ(1, sigma*k*y)+BesselY(1, sigma*k*y))/(beta2*BesselJ(2, sigma*k*y)+BesselY(2, sigma*k*y))-(BesselY(2, y)*BesselJ(1, k*y)-BesselJ(2, y)*BesselY(1, k*y))/(BesselY(2, y)*BesselJ(2, k*y)-BesselJ(2, y)*BesselY(2, k*y)), y = 2*x01 .. 4*x01);
x22 := fsolve(sigma*(beta2*BesselJ(1, sigma*k*y)+BesselY(1, sigma*k*y))/(beta2*BesselJ(2, sigma*k*y)+BesselY(2, sigma*k*y))-(BesselY(2, y)*BesselJ(1, k*y)-BesselJ(2, y)*BesselY(1, k*y))/ (BesselY(2, y)*BesselJ(2, k*y)-BesselJ(2, y)*BesselY(2, k*y)), y = 4*x01 .. 6*x01);
x31 := fsolve(sigma*(beta3*BesselJ(2, sigma*k*y)+BesselY(2, sigma*k*y))/(beta3*BesselJ(3, sigma*k*y)+BesselY(3, sigma*k*y))-(BesselY(3, y)*BesselJ(2, k*y)-BesselJ(3, y)*BesselY(2, k*y))/ (BesselY(3, y)*BesselJ(3, k*y)-BesselJ(3, y)*BesselY(3, k*y)), y = 3*x01 .. 5*x01);
x41 := fsolve(sigma*(beta4*BesselJ(3, sigma*k*y)+BesselY(3, sigma*k*y))/(beta4*BesselJ(4, sigma*k*y)+ BesselY(4, sigma*k*y))-(BesselY(4, y)*BesselJ(3, k*y)-BesselJ(4, y)*BesselY(3, k*y))/ (BesselY(4, y)*BesselJ(4, k*y)-BesselJ(4, y)*BesselY(4, k*y)), y = 4*x01 .. 6*x01);
TheError := $(1/9)*(x02/x01-3)^2+(1/4)*(x11/x01-2)^2+(1/16)*(x12/x01-4)^2+(1/25)*(x03/x01-5)^2+(1/9)*(x21/x01-3)^2+(1/25)*(x22/x01-5)^2+(1/16)*(x31/x01-4)^2+(1/25)*(x41/x01-5)^2$;
if (0 <= TheError < 1) = true **then return** TheError **else return** undefined
end if end proc;

Error values for each permutation
> Error := map(‘@‘(Err1, op), comb);

Minimum error for set
> MinError := min[defined](Error);

Return parameters corresponding to minimum
> member(MinError, Error, ’p’);
> ParametersMin := comb[p];

C.4 Minization in the Variational Method

This program find the value of x_{22} .

Define Parameters
> $\Delta := 0$; n := 2; k := 0.4; $\sigma := 3.125$;
> scale := 1+4*Δ^2*s^2+4*Δ*s*cos(θ)+6*Δ^2*s^2*cos(2*θ);

Eliminating Parameters using the Boundary Conditions
> $b_2 := -b_4$;
> $a_2 := b_2 + b_4 * k^2 + c_2 * ln(k) + c_4 * k^2 * ln(k) - a_4 * k^2 - a_6 * k^4 - a_8 * k^6$;
> c_2 := 2*($b_2 + b_4 * k^2 + c_4 * k^2 * ln(k) - a_4 * k^2 - a_6 * k^4 - a_8 * k^6$) + $4 * a_4 * k^2 + 6 * a_6 * k^4$ + $8 * a_8 * k^6 + 2 * b_4 - 4 * b_4 * k^2 - c_4 * (4 * k^2 * ln(k) + k^2)$;

Eliminating Parameter using Orthogonality
> $b_4 := -0.03814950200 * a_8 - 0.1615789455 * a_6 - 0.5178547004 * a_4 - 0.5112898471 * c_4$;

Functions for ψ_1, ψ_2
> $\psi_1 := (a_2 * s^2 + a_4 * s^4 + a_6 * s^6 + a_8 * s^8) * \cos(n * \theta)$;
> $\psi_2 := (b_2 * s^2 + b_4 * s^4 + c_2 * s^2 * ln(s) + c_4 * s^4 * ln(s)) * cos(n * \theta)$;

The equation for x^2
> d := int(s*((diff(ψ_1, s))^2+(diff(ψ_1, θ))^2/s^2), [s = 0 .. k, θ = 0 .. 2*Pi]);
> e := int(s*((diff(ψ_2, s))^2+(diff(ψ_2, θ))^2/s^2), [s = k .. 1, θ = 0 .. 2*Pi]);
> f := σ^2*(int(s*ψ_1^2*scale, [s = 0 .. k, θ = 0 .. 2*Pi]));
> g := int(s*ψ_2^2*scale, [s = k .. 1, θ = 0 .. 2*Pi]);
> h := (d+e)/(f+g);

Minimization of x^2
> with(Optimization); Normalizer := simplify; Minimize(h, iterationlimit = 10000);

The value of x
> sqrt(26.8591158221655206);

Appendix D

CD Contents

Filename: perfectharmonicity.wav
This file contains the sound created if all the harmonics were in integer multiples.

Filename: ordinarydrum.wav
This is the sound of the harmonics produced by the ordinary drum, up to the 6^{th} harmonic.

Filename: 2density6th.wav
This file contains the sound produced by the best agreement with perfect harmonicity for the 2-density model if the ψ_{03} root is placed at the 6^{th} harmonic.

Filename: perfect3density6th.wav
This file contains the sound produced by the best agreement with perfect harmonicity for the 3-density model if the ψ_{03} root is placed at the 6^{th} harmonic.

Filename: perfect3density5th.wav
This is the sound produced by the best agreement with perfect harmonicity for the 3-density model if the ψ_{03} root is placed at the 5^{th} harmonic. There is a notable improvement over the 6^{th} harmonic case.

Filename: experimental.wav
This file contains the sound created by the harmonics that were experimentally found by Ramakrishna and Sondhi.

Filename: model3densitylimited.wav
This is the sound produced by the best agreement of the 3-density model with the experimental values for the right-handed tabla.

Filename: model3densityminimal.wav
This is the sound produced by the best agreement with the experimental values for the 3-density model when the relative density and radial ratio of the syahi and membrane are within the physical limits of the right-handed tabla.